

MICROPROCESSOR CONTROLLED TEMPERATURE PROFILE GENERATOR FOR SEMICONDUCTOR EXPERIMENTS

by

UTPAL KANTI MUKHOPADHYAYA



DEPARTMENT OF ELECTRICAL ENGINEERING
INDIAN INSTITUTE OF TECHNOLOGY, KANPUR

APRIL, 1985

TH
CE/1985/m
M 896m

EE

1985

M

MUK

MJC

MICROPROCESSOR CONTROLLED TEMPERATURE PROFILE GENERATOR FOR SEMICONDUCTOR EXPERIMENTS

**A Thesis Submitted
In Partial Fulfilment of the Requirements
for the Degree of
MASTER OF TECHNOLOGY**

**by
UTPAL KANTI MUKHOPADHYAYA**

**to the
DEPARTMENT OF ELECTRICAL ENGINEERING
INDIAN INSTITUTE OF TECHNOLOGY, KANPUR
APRIL, 1985**

17 JUN 1965

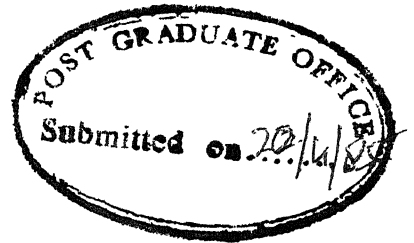
117 250000

87564

EE-1985-M-MUK-MIC

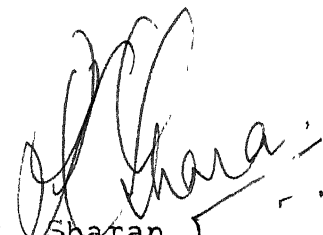
DEDICATED
TO
MY PARENTS.

CERTIFICATE



This is to certify that this thesis entitled
'MICROPROCESSOR CONTROLLED TEMPERATURE PROFILE GENERATOR
FOR SEMICONDUCTOR EXPERIMENTS' by U.K. MUKHOPADHYAYA
has been carried out under my supervision and has not
been submitted elsewhere for a degree.

April, 1985


(R. Sharan)
Professor
Department of Electrical Engineering
Indian Institute of Technology
KANPUR 208016, INDIA

208016
This is to certify that
27/4/85

ACKNOWLEDGEMENT

I wish to take this opportunity to express my deepest sense of gratitude to my supervisor, Dr. H. Sharan for his valuable guidance and concern at every stage of this thesis.

I am also grateful to Dr. R.N. Biswas and Dr. J. Narain for their invaluable time and suggestions during the course of this work.

I take this opportunity to thank Research Engineers Mr. B. Nandi, Mr. P. Bandyopadhyay and Mr. S.S. Bandyopadhyay for their friendly help.

Thanks are also due to all my colleagues in particular Mr. R.P. Gupta, Capt. A.K. Das, S. Sanyal, S.P. Yeotikar, S.K. Mondal, P. Thakur, S. Chandrasekhar and Mr. C.S. Mukherjee for nice company and enthusiastic help towards this project.

Last but not the least, I acknowledge the excellent typing done by Mr. J.S. Rawat.

UTPAL KANTI MUKHOPADHYAYA

ABSTRACT

Various semiconductor experiments, performed to characterize the semiconductor materials and devices, require programmed heating profiles for heating the specimens. Temperature controllers capable of generating programmed heating rates are difficult to design. Some efforts were made to realize controller generating simple linear heating rates. But they all suffered from (a) inaccuracy of rates (b) narrow range (c) lack of smoothness in temperature variation. In this thesis, a simple and versatile microprocessor controlled temperature profile generator has been realized. The controller is capable of generating both linear and hyperbolic heating profiles.

For generating ramp rates, a closed-loop control scheme has been used, where temperature rate instead of temperature is used as the feedback signal. Temperature rate rather than temperature becomes the controlled variable.

For hyperbolic rates, first a piecewise linear approximation of the non-linear curve is made. Then the ramp scheme itself is used to realize those linearized parts.

To ensure an EMI-free heating, zero-voltage switching technique has been adopted.

TABLE OF CONTENTS

	Page
CHAPTER 1 INTRODUCTION	1
CHAPTER 2 SCHEMES FOR GENERATING TEMPERATURE PROFILES	5
2.1 Schemes	5
2.2 Important aspects in the Design of Temperature Controllers	8
CHAPTER 3 ACTUAL SCHEME FOR GENERATING TEMPERATURE PROFILES	10
3.1 Types of Temperature Profiles generated	10
3.2 Actual Scheme	11
3.2.1 Thermochuck	11
3.2.2 Thermocouple	13
3.2.3 Power Transformer	13
3.2.4 A.C. Power Controller	13
3.2.5 Interrupt Generator	16
3.2.6 Amplifier Circuitry	16
3.2.7 Temperature Monitoring	21
3.2.8 A/D Converter	21
3.2.9 Microprocessor	22
3.3 Algorithm	24
3.3.1 Ramp Mode	24
3.3.2 Hyperbolic Mode	33

CHAPTER 4	EXPERIMENTAL DETERMINATION OF MOBILE ION CONTAMINATION IN MOS CAPACITORS	40
4.1	Experiment	41
4.2	Results and Discussion	47
4.3	Conclusion	51
CHAPTER 5	RESULTS AND DISCUSSION	52
5.1	Ramp Data	52
5.2	Hyperbolic Data	58
5.3	Limitations	60
CHAPTER 6	CONCLUSION	63
APPENDIX I	: Calibration Procedure of the Thermocouple Amplifier Circuits for Cold -Junction Compensation	67
APPENDIX II	: Operating Instructions for the Temperature Controller	69
REFERENCES		74

LIST OF FIGURES

Fig. No.	Title	Page
2.1	Old Scheme for generating Ramp rate of heating	7
2.2	New Scheme for generating Ramp rate of heating	7
2.3	Scheme for generating constant temperature	7
3.1	Block schematic of the microprocessor controlled temperature profile generator	12
3.2	Circuit diagram of A.C. power Controller	15
3.3	Interrupt Generator	17
3.4	Thermocouple amplifier circuitry	19
3.5	Open and closed loop response of the controller	26
3.6	Flowchart showing the main programme for Ramp Mode	28
3.7	ISS programme for Ramp Mode	29
3.7(contd.)	ISS programme for constant temperature Mode	30
3.8	Main programme for hyperbolic heating rate	35
3.9	ISS programme for hyperbolic heating rate	36
4.1	Structure of a n-type MOS capacitor	42

Fig. No.	Title	Page
4.2	Capacitances associated with n-type MOS capacitor	42
4.3	High frequency as well as low frequency C-V curves of MOS capacitors	43
4.4	Experimental set-up for determining the density of mobile ions in MOS capacitors	45
4.5	High frequency C-V curves obtained as a result of bias-temperature aging	46
4.6	Oxide charges present in practical MOS capacitors	49
5.1	T-t output of the controller in ramp mode	53
5.2	T-t output of the controller in hyperbolic mode	59

CHAPTER 1

INTRODUCTION

The characterization of semiconductor materials and devices is needed to characterize the process through which they have been fabricated or for their proper utilization in circuits. There are several characterization methods which depend on the manipulation of temperature across the material or the device. Typical examples of such methods are, determination of mobile ion contamination in oxide layers of MOS devices, Deep Level Transient Spectroscopy (DLTS), Thermally Stimulated capacitance or current transients etc. Basically, there are two systems of temperature variation which are utilized in this kind of study. Let us call them Type I and Type II. In Type I system, the rate (or profile) of heating between the initial and final temperature, at which the sample or specimen temperature should be heated up, is of no importance; whereas in Type II system, the profile of heating is important. Examples for Type I system include, detection of the density of mobile ions in oxide layers of MOS devices, by subjecting the device to bias-temperature stressing. This type of experiment does not call for a programmed heating profile. The device needs to be heated up to some final

temperature with a bias voltage applied across it. The exact profile of heating is immaterial [1]. Examples for Type II system include experiments like Thermally stimulated conductivity measurements etc. The theories of TSC (Thermally Stimulated Conductivity) assume that sample temperature varies linearly with time [2]; although more general theories have recently been formulated and calculations have been made for a hyperbolic heating rate schedule ($\frac{1}{T} \propto t$) [3].

Temperature controllers capable of generating Type I system of heating, are commercially available. Controllers of Type II are more difficult to design. However, some efforts have been made to design Type II controllers; starting from manual techniques of controlling temperature by means of electromechanical cams to analog \dot{T} -T controllers, capable of generating ramp as well as constant temperature heating, have been realized. But they all suffered from (a) accuracy of rates (2) lack of smoothness in temperature variation (3) difficulties in introducing non-linear temperature variation.

A microprocessor controlled temperature profile generator provides a good solution. It circumvents all the drawbacks associated with the existing analog controllers

and makes the controller highly flexible and versatile. In the present work, a microprocessor controlled Temperature Profile Generator, capable of generating ramp as well as hyperbolic rate of heating, has been realized.

Chapter 2 of the thesis contains a brief discussion of some of the schemes of generating temperature profiles, that were developed earlier. The important design factors for satisfactory realization of a temperature controller, have also been pointed out.

The actual scheme used to realize the microprocessor controlled temperature controller has been elaborated in Chapter 3. A block schematic has been presented. The circuits belonging to the important blocks have been explained. The flow charts given there help in understanding the 'algorithms' used to realize the linear as well as the hyperbolic heating profiles. A closed-loop control scheme has been used to realize both the profiles. In ramp mode, the derivative of temperature ($\frac{\Delta T}{\Delta t}$) is compared periodically with the desired ramp rate and depending on the amount and direction of error, a.c. power controller is actuated in the right direction to minimize this error. In constant temperature mode, temperature itself becomes the feedback signal to be compared with the reference. A simple 'Proportional Control'

is used to maintain constant temperature. A hyperbolic heating profile in accordance with the equation $\frac{1}{T} \alpha t$, is realized by employing the ramp scheme itself, after making a piecewise linear approximation of the hyperbolic curve.

Systems providing automated measurement capability are highly useful in process development as well as on-line production and quality control applications. In Chapter 4, an experiment, for determining the density of mobile ion contamination in MOS capacitor, has been performed with the help of commercial controllers. The results have been analyzed and discussed.

In Chapter 5, a set of curves for both linear as well as hyperbolic profiles, have been shown. They have been obtained with the help of our controller. The deviations from the expected results, the reasons for the discrepancies and also the limitations of our controller have been discussed.

Chapter 6 is the concluding chapter. Here a number of suggestions for overcoming the limitations of the present temperature profiles have been given.

CHAPTER 2

SCHEMES FOR GENERATING TEMPERATURE PROFILES

The need for generating different heating profiles, to which a device under test (DUT) is subjected during an experiment, was stressed in the previous chapter.

Schemes for generating these profiles, particularly linear and hyperbolic ones, are briefly touched upon here.

2.1 SCHEMES:

During earlier periods, electromechanical cams and potentiometer operated programme controllers were employed to realize a linear rate of rise of temperature [4].

This manual technique of achieving a constant heating rate, was followed by the design of a Temperature Controller, which comprised of a ramp generator, a summing amplifier and a SCR gating amplifier. The controller operated only in the range between 90°K and 300°K . These analog integrator type programmable controllers required highly stable, expensive components to reduce drift and were not found suitable for extremely long time-base ramps, because of eventual voltage decay across the integrating capacitor [5].

An inexpensive programmable temperature controller which employed a digitally generated voltage ramp for controlling temperature-time relationship, was realized [6]. The instrument provided only seven heating or cooling rates from 0.25 to 8°C/min over a temperature span from -40°C to +20°C. Basically comprised of a digitally controlled ramp voltage generator, a thermistor temperature sensing circuit, a differential comparator, and a \wedge ^{triac} a.c. switching circuit, the system had a power capacity of about 1000 watts.

All these temperature controllers follow a closed-loop control scheme as shown in Fig. 2.1. A feedback signal proportional to temperature ^{is} nulled against a reference signal. This reference signal itself used to have the desired time dependence. The amplified difference between the reference and the feedback, is used to power the heater. This scheme suffers from (a) accuracy of rates and (b) lack of smoothness in temperature variation.

Another scheme was proposed [7], in which instead of nulling the feedback signal (proportional to temperature) against a ramp, the derivative of temperature was nulled against a fixed ramp rate reference, shown in Fig. 2.2. Thus temperature rate rather than temperature was made the controlled variable. The scheme also had a facility to



FIG.2.1 OLD SCHEME FOR GENERATING RAMP RATE OF HEATING

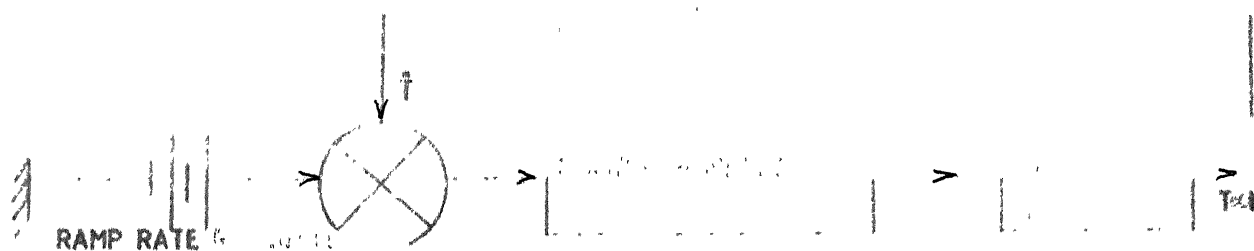


FIG.2.2 NEW SCHEME FOR GENERATING RAMP RATE OF HEATING.

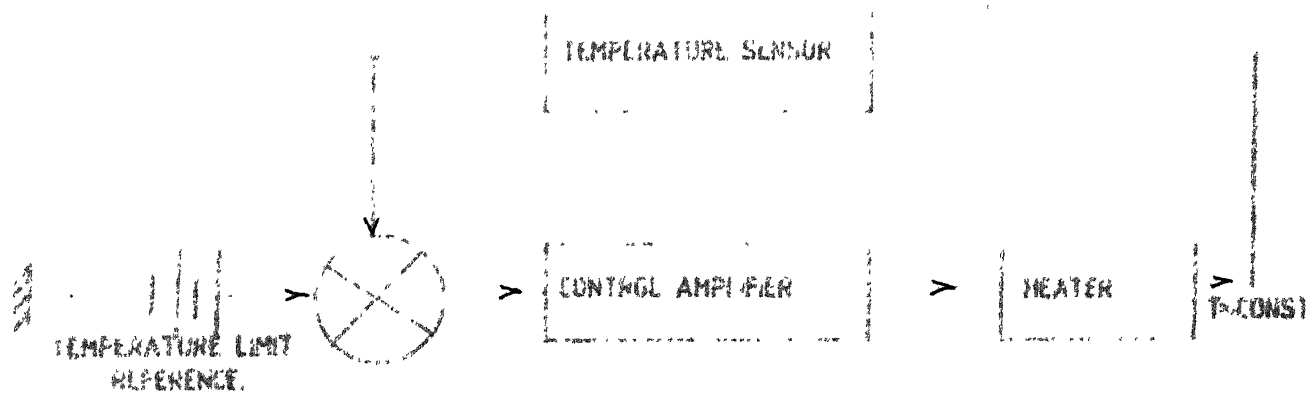


FIG.2.3 SCHEME FOR GENERATING CONSTANT TEMPERATURE

switch from ramp mode (\dot{T} mode) to constant temperature mode (T). The scheme in constant temperature mode is shown in Fig. 2.3.

Based on the schemes as depicted in Fig. 2.2 and Fig. 2.3, a microprocessor controlled temperature profile generator has been proposed in the present work. Employing the same scheme alongwith a piecewise linear approximation technique, a hyperbolic heating profile has also been realized. The use of microprocessor has made the controller highly flexible and versatile.

2.2 IMPORTANT ASPECTS IN THE DESIGN OF TEMPERATURE CONTROLLERS:

For satisfactory realization of a reliable temperature controller, the important aspects that should be considered are:

a) Sensitive, low loss heater assembly:

The design, construction and characterization of a sensitive, low loss heater play an important role in the design of any temperature controller. An extensive discussion regarding variable temperature wafer chucks is available in Ref. [8]. Both the static (isothermal) and dynamic thermal characteristics of the chucks become important in the design of controller. The chuck assemblies

should also have facilities (1) to monitor chuck temperature and (2) to probe wafers kept over them for measurement purpose.

b) Noise and transient free heating of heater assemblies:

A d.c. power controller is desirable for ensuring noise and transient free heating of the system, but it is difficult and expensive to realize d.c. controllers having power capability of about 500 watts. A.C. power controllers employing thyristors do not suffer from power limitation. But the usual firing angle control technique for controlling load power, results in interference problems. These 'Radio frequency interferences' are generated due to switching of load current from a zero value to a value limited by the load itself in a few microsecs. They are eliminated by adopting a technique known as 'Zero-voltage Switching', in which Thyristors are triggered always at the zero crossing of the applied a.c. voltage. Power is applied to the load in terms of integral number of a.c. cycles and power is controlled by modulation of the duty cycle.

CHAPTER 3

ACTUAL SCHEME FOR GENERATING TEMPERATURE PROFILES

Various schemes for generating temperature profiles have already been discussed in the previous chapter. The actual scheme, which has been implemented, is being elaborated here.

3.1 TYPES OF TEMPERATURE PROFILES GENERATED:

Two different types of temperature profiles have been realized here.

(1) Linear variation of temperature with time, at various rates (starting from 20°C/min upto 90°C/min), with a facility to stop or rather cross over from ramp mode to constant temperature mode, at any point between ambient and 300°C (which is the highest temperature our heating element should not be operated beyond).

(2) Hyperbolic variation of temperature with time satisfying the equation

$$\frac{1}{T} = \frac{1}{T_0} - at \quad (3.1)$$

where, T = Actual temperature in °C

T_0 = Initial temperature (the ambient itself) in °C

a = constant of proportionality in $^{\circ}\text{C}/\text{min}$

varying from 0.01 to 0.001

and t = Time in minutes

Hyperbolic heating scheme does not have the facility to cross over from hyperbolic to constant temperature mode.

3.2 ACTUAL SCHEME:

The block diagram schematics for realizing the two types of temperature profiles have been shown in Fig. 3.1.

The blocks within the dotted area have been designed and fabricated, whereas the remaining blocks have been commercially available.

Details of each block are enumerated below:

3.2.1 Thermochuck:

The thermochuck we have used, is model TP36A made by Temptronic Corporation, U.S.A. Its surface is copper plated with 300 microinches of nickel and 200 microinches of 24K Gold. The surface has got a small hole at its centre which ensures reliable contact between the wafer surface and thermochuck surface under vacuum. The heating element of the chuck has got a nominal resistance value of about 35 ohms; wattage $\frac{1}{2}$ of 500 watts and it operates on 115v A.C. 50/60 Hz.

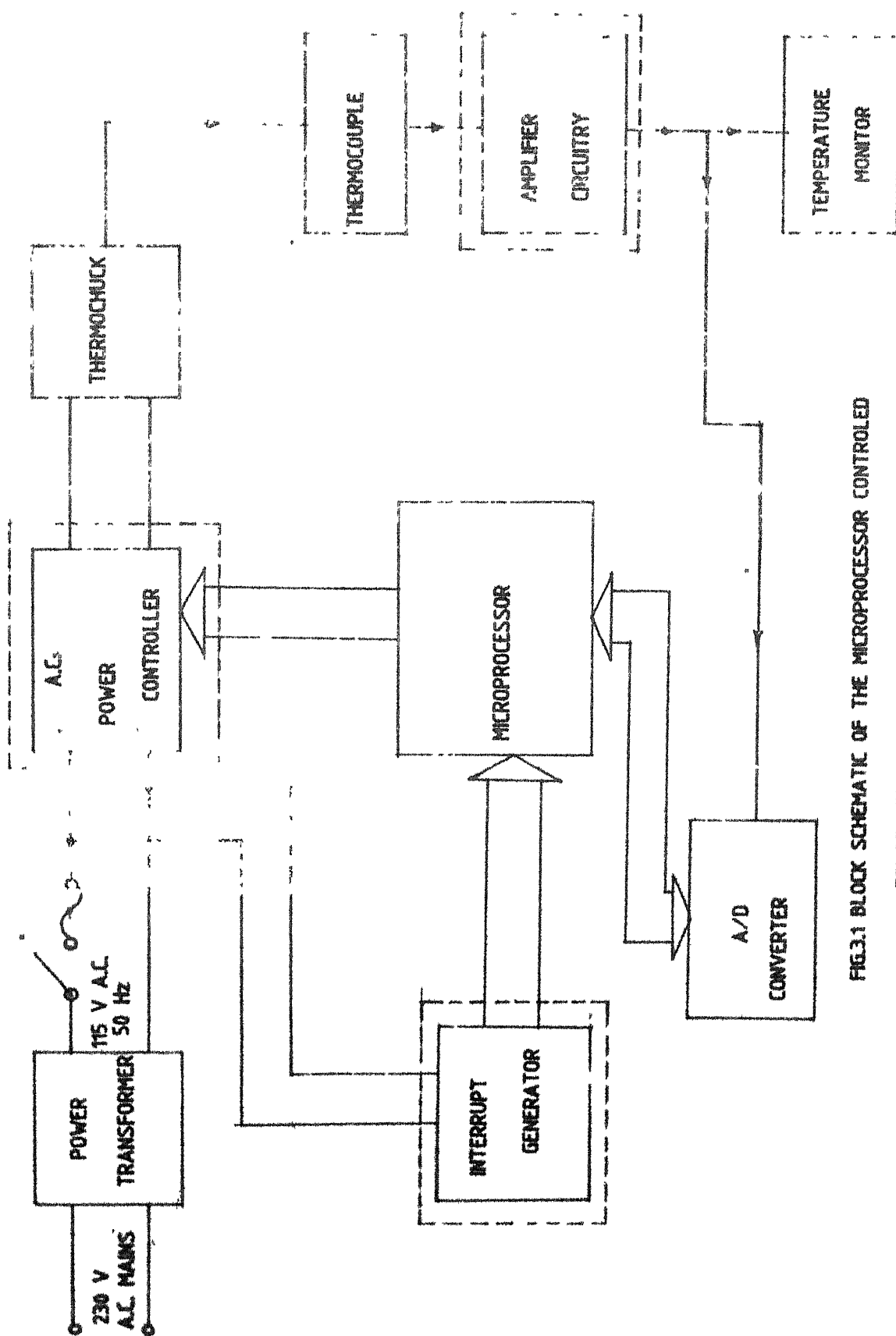


FIG.3.1 BLOCK SCHEMATIC OF THE MICROPROCESSOR CONTROLLED
TEMPERATURE PROFILE GENERATOR.

3.2.2 Thermocouple:

An iron-constantan thermocouple embedded inside the chuck assembly, has been provided mainly to monitor the chuck temperature. The two lead-outs of the thermocouple are used for extracting temperature information as well as for further processing of the thermosignals. The volt - outputs vs. temperature (in $^{\circ}\text{C}$) characteristics of the Iron-Constantan i.e. Type J thermocouple (useful in the range between -184°C and 760°C) shows a good linearity between ambient and 300°C . This thermocouple has a good long term stability and a quite fast response.

3.2.3 Power Transformer:

A step-down power transformer of 500 VA has been provided to get 115 A.C. supply which is necessary to heat the thermochuck.

3.2.4 A.C. Power Controller:

One of the important blocks of the solid-state temperature controller is the A.C. Power Controller. It was stressed earlier that we need EMI-free heating. Zero-point switching technique [9], which controls sine-wave power in such a way that either complete cycles or half cycles of the power supply voltage are applied to the load, has been

employed to ensure EMI-free heating. A typical circuit diagram employing thyristors as zero-point switches, are shown in Fig. 3.2.

If an SCR is turned on with an anode voltage as low as 10 volts and with a load of just a few hundred watts, then large EMI will result. The thyristor, which needs to be turned on at the start of each positive alternation, must receive a gate drive exactly at the zero-crossing of the applied voltage. Because of this exact-timing requirement, pulse type thyristor triggering is usually impracticable since even small timing drifts will result in off-zero switching or possibly no switching at all. The problem is circumvented by providing the gate signal before the zero crossing itself. The phase-shift network comprising of C_1 and R_1 supplies a 90° shifted sine-wave gate signal to the SCR Q_2 . Since only one thyristor (Q_2) can be controlled from this phase shifted signal, a slaving circuit becomes necessary to control the other SCR (Q_3) to get full-wave power control. Q_2 is usually known as Master SCR and Q_3 as slaving SCR. Each time Q_2 applies a positive half cycle of power to the load, it energizes the slave circuit (as shown dotted), which will then fire Q_3 and apply the following negative half cycle of power to the load. Hence load power

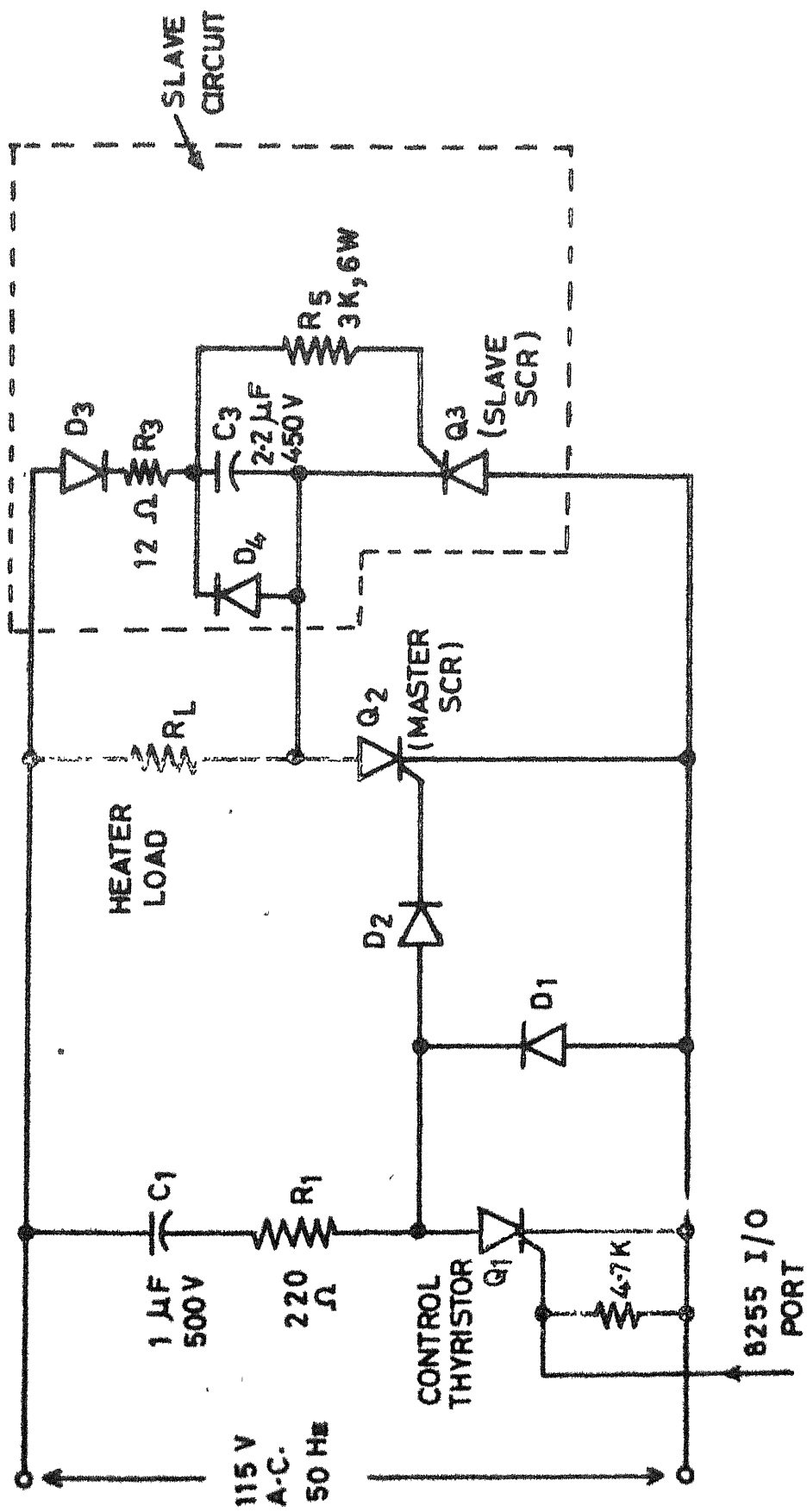


FIG.3.2 CIRCUIT DIAGRAM OF A.C. POWER CONTROLLER .

is completely controlled on a full-wave basis by controlling the master SCR Q_2 . A small SCR Q_1 , known as 'control SCR', shunts the gate signal of Q_2 to ground, when no load power is required. This 'control SCR' is controlled by means of an I/O port pin of 8255 chip of a μ P system (which will be discussed later).

3.2.5 Interrupt Generator:

The importance of this block (shown in Figs. 3.1 and 3.3) will become evident in the later part of discussion when we will discuss the algorithm used for generating temperature profiles. A block schematic used for generating interrupts is shown in Fig. 3.3.

A small sample of the same a.c. sinewave (applied to the load) is fed to an optocoupler for proper isolation. The square-wave output (TTL compatible) is fed to a hex inverter buffer, after which it is differentiated by an ordinary RC network. The negative spikes are blocked by means of a diode and positive spikes of five volt amplitude spaced at an interval of 20 msec (i.e. one a.c. cycle apart) are fed to RST 6.5 pin of 8085.

3.2.6 Amplifier Circuitry:

The thermo-e.m.f.'s of the Iron-Constantan thermo-couple are basically low level (of the order of few hundred

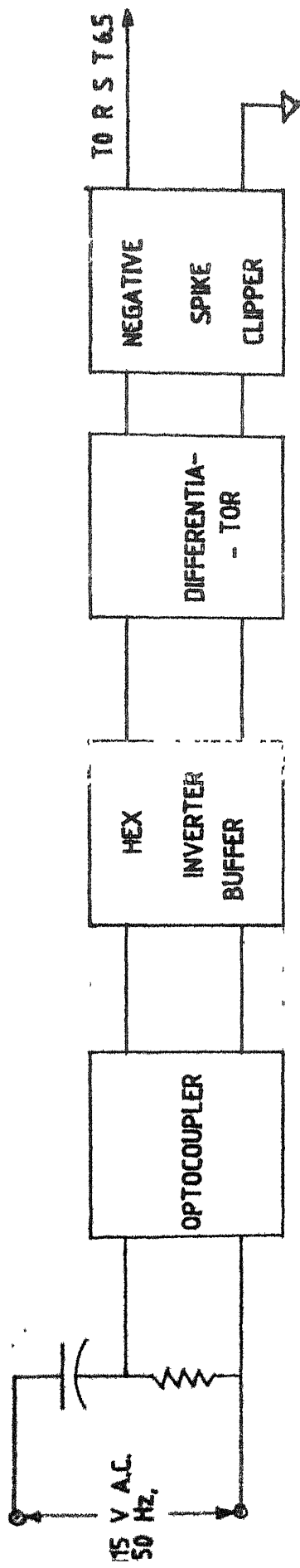


FIG. 3.3 INTERRUPT GENERATOR .

microvolts), and also these devices are low impedance sources. Proper signal conditioning is required before these signals can be utilized for control purposes. Fig. 3.4 shows the circuit diagram of an amplifier which ensures high input impedance, low offset and drift, low non-linearity, stable gain and low effective output impedance. The above circuit also provides a kind of 'cold junction compensation' for the thermocouple.

The output voltage of thermocouple is proportional to the temperature difference between the measuring end and the reference end which (ideally should be a 0°C ref), normally is the ambient temperature itself. A variation in ambient temperature, i.e. a variation in reference junction temperature will introduce a kind of error in measurement and needs to be automatically compensated. Fig. 3.4 shows the circuit which ensures that.

LM 321 is an instrumentation amplifier.

In conjunction with LM308A, this forms a precision low-drift op-amp giving a direct reading output in $10\text{ mV}/^{\circ}\text{C}$. LM321 is specifically designed for use with general purpose op-amps to obtain drifts of $1\text{ }\mu\text{V}/^{\circ}\text{C}$. When the offset voltage is nulled, the drift is also nulled. There is a theoretical relationship between the offset voltage and drift, when the

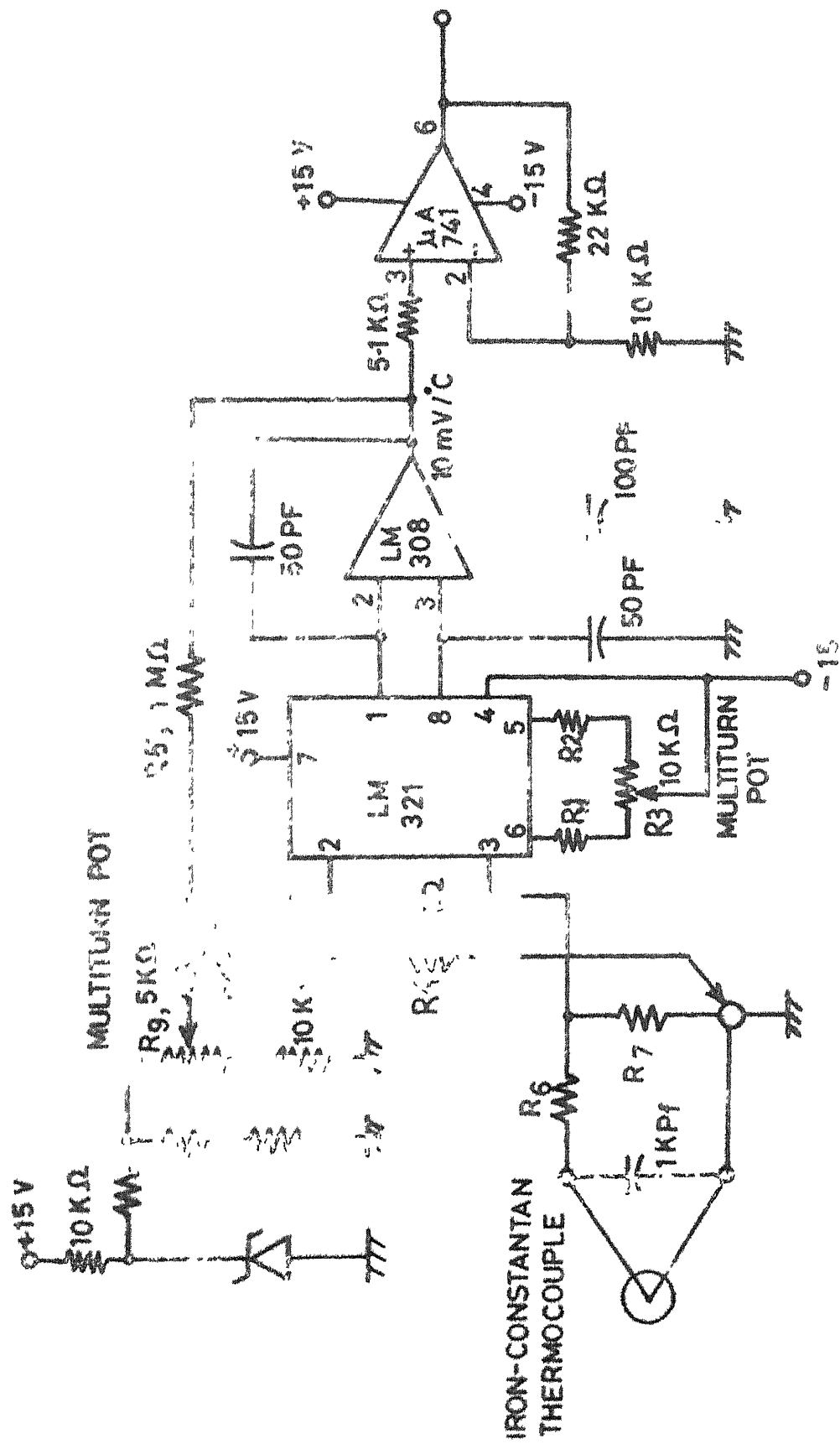


FIG. 3.4 THERMOCOUPLE AMPLIFIER CIRCUITRY

offset is not nulled to zero. The drift of the amplifier is then used to compensate the thermocouple for ambient temperature variations [10]. Drift is given by,

$$\frac{dV_{OS}}{dT} = \frac{V_{OS}}{T}$$

where V_{OS} = offset voltage

T = temperature in $^{\circ}K$

Resistors R_1 , R_2 and R_3 set the operating currents of the pre-amplifier and R_3 is used to adjust the offset. The offset and drift are amplified by the ratio of feedback resistors R_4 and R_5 and appears at the output. R_6 and R_7 attenuate the thermocouple's output to $10 \mu V/^{\circ}C$ to match the amplifier drift and set the scale factor at $10 mV/^{\circ}C$.

The zener provides a reference for offsetting the output to read directly in $^{\circ}C$.

The maximum temperature is $300^{\circ}C$; therefore the maximum output voltage at the output of LM308 will be 3 volts (at $10 mV/^{\circ}C$). Now this 3 volt is not sufficient to drive the A/D converter, which actually serves as an interface between the analog world and digital world. Another stage gain (non-inverting) of about 3.2 has been incorporated by means

of an op-amp μA 741 so that max. possible output now becomes 9.6 volt, enough to drive ^{the} \angle A/D converter to give satisfactory digitization of the analog signal.

The amplifier needs to be calibrated, for cold-junction compensation Appendix I gives procedure of calibration.

3.2.7 Temperature Monitoring:

A digital multimeter (DMM) (by Keithley) is connected at the output of the Op-amp LM308 for monitoring the chuck temperature. Because the output of LM308 is obtained in terms of 10 mV/ $^{\circ}C$, the temperature is measured by multiplying the displayed voltage in DMM (for a setting of DCV, 20V) by a factor of 100.

A Hewlett-Packard X-Y plotter is connected at the output of the op-amp μA -741 to obtain hard copies of the variation of temperature with time. The X-axis of the recorder is driven by a suitable RAMP.

3.2.8 A/D Converter:

After proper conditioning of the thermoelectric emf (to a level of max. 10V) it is fed to an A/D converter, for the sake of digitization. AD574, a 12-bit, fast, successive approximation type A/D converter, with 3-state output buffer circuitry for direct interface to the microprocessor, is used for the purpose.

The 12-bits of output data (which can be read either as one 12-bit word or as two 8-bit bytes) are taken through two I/O ports of 8255 PPI chip of the microprocessor system.

Two analog input pins are available, one with a voltage span of 0 to +10V and the other from 0 to +20V. The former one is connected resulting in LSB nominal value of about 2.44 mV.

The A/D converter chip contains on-chip logic to provide conversion initiation and data read operations from signals commonly available in microprocessor systems. Control pins like \overline{CS} (chip select), \overline{CE} (chip enable) and R/\overline{C} (data read or convert) etc. are all controlled by means of I/O port pins of 8255 chips.

3.2.9 Microprocessor:

The heart of the entire control system is a microprocessor 8085, along with its various other auxiliaries. We used a microprocessor kit VMC-85, a single board development kit configured around 8085, as the central processing unit.

The kit communicates with the outside world through a keyboard having 28 keys and seven-segment hexadecimal display. The 8279 chip, General purpose programmable keyboard and display I/O interface device, provides a scanned interface to 28 contact key matrix and also a scanned display interface

for the six seven-segment displays. User is required to enter the various parameters of temperature-profiles, through this keyboard.

VMC-85 provides a total of 4K bytes of RAM using 2114 chips and 12K bytes ROM using 2716 EPROM chips. The ON-board resident system monitor software is supplied with two EPROMS, and we have stored our software (for generating temperature profiles) in the remaining two EPROMS (Address locations 1880 for linear, and IBBO for hyperbolic).

The input/output structure of VMC-85 provides a total of 46I/O lines using two 8255 PPI chips. These basically act as general purpose I/O components to interface peripheral equipments to the system bus. For example, A/D converter, control thyristor of A.C. power controller, interrupts etc. all are connected through these I/O chips. The most important advantage is that, functional configuration of 8255 is programmed by the system software, not by any external logic.

A 16-bit programmable timer/counter 8253 has also been provided. It also has programmable interrupt controller alongwith Trap, RST 7.5, RST 6.5 and RST 5.5.

Apart from the facilities mentioned above, which are important for our purpose, facilities like Audio cassette

Interface, Teletype, HTL and CMT interfaces have also been provided with VIC-85 kit.

3.3 ALGORITHM:

Having discussed the different blocks in Fig. 3.1, we now present the 'algorithm' followed for generating both linear as well as hyperbolic temperature profiles. The flow charts are shown in Figs. 3.6 - 3.9. The entire scheme is vector interrupt (RST 6.5) controlled.

There are two different programmes for the two types of temperature profiles; each one having one main programme and one Interrupt Service Subroutine (ISS). The main programme for ramp mode of heating is stored in EPROM from location 1830 H onwards and its ISS from 1A80H; whereas for hyperbolic heating profiles, main programme has been stored from 1B80 H and its ISS from 1D20H onwards.

A set of operating instructions for generating the desired temperature profiles has been given in Appendix II.

3.3.1 RAMP Mode:

If a constant power is applied to the heater load, the thermochuck temperature starts rising, initially in a linear fashion, but later slowly drooping away from the

initial rate (shown in Fig. 3.5). This initial rate of rise depends on the power applied i.e. on the 'duty cycle'. Our concern is to ensure a constant rate of rise of temperature, as shown by the dotted curve in Fig. 3.5. A closed-loop control scheme has been used, where frequently a check is made with the desired ramp rate and depending on the error (whether positive or negative) between the desired rate and the actual rate, a 'correction' is applied to the duty cycle resulting in either increase or decrease in duty cycle. The other important aspect is that, by means of thermocouple we monitor the temperature, not the rate. Therefore, from two different temperature readings at two different specified instants of time, $\frac{\Delta T}{\Delta t}$ is computed out which is then compared with the desired $(\frac{\Delta T}{\Delta t})$.

For constant temperature mode, after the termination of ramp mode, a simple 'proportional control' is employed. If the actual temperature of the chuck is above the set point value, i.e. above the desired final temperature, power to the load is turned off. On the other hand, if it is below the set point and within the 'proportional band', a power, proportional to the amount of error, is applied to the load.

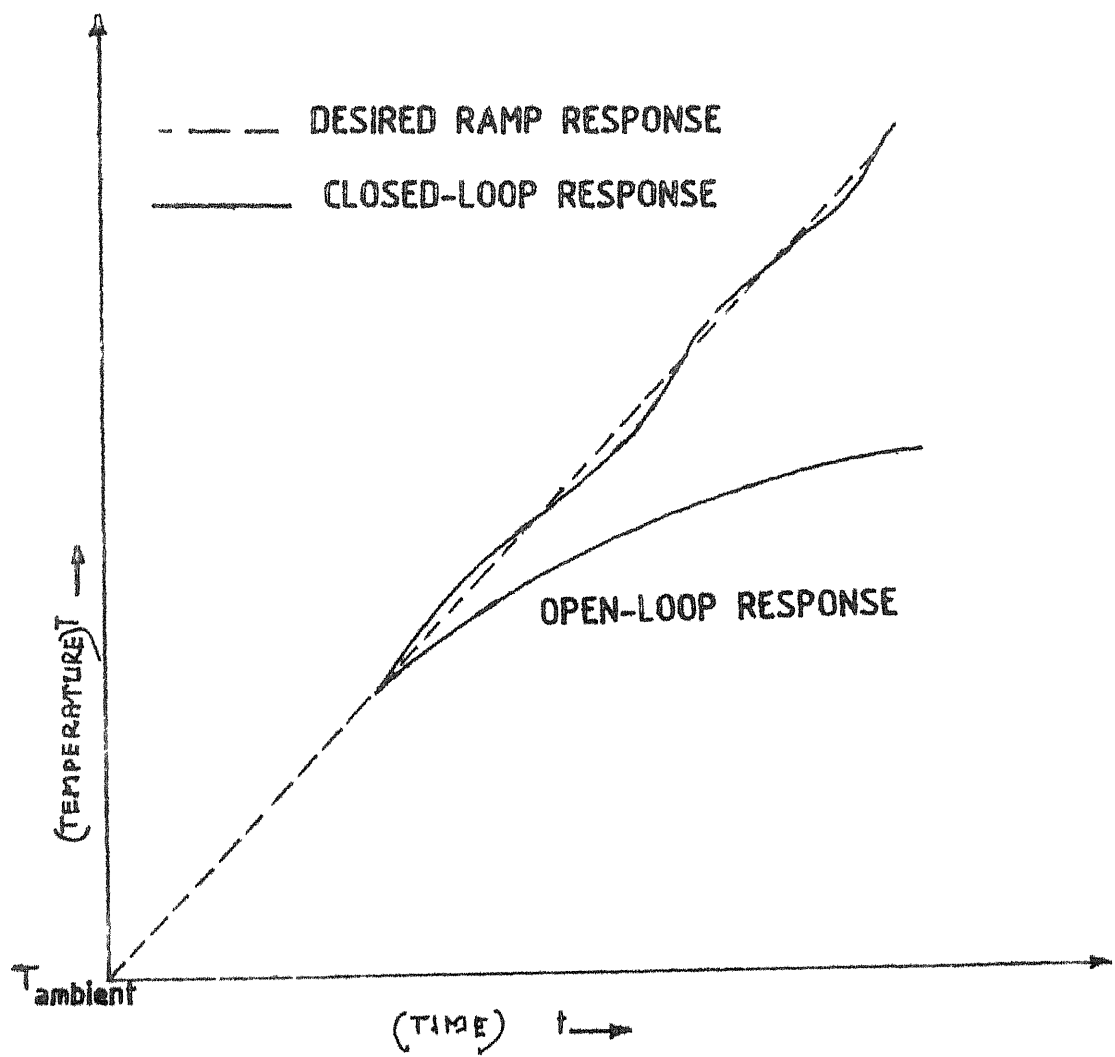


FIG.3.5 OPEN AND CLOSED LOOP RESPONSE OF THE CONTROLLER

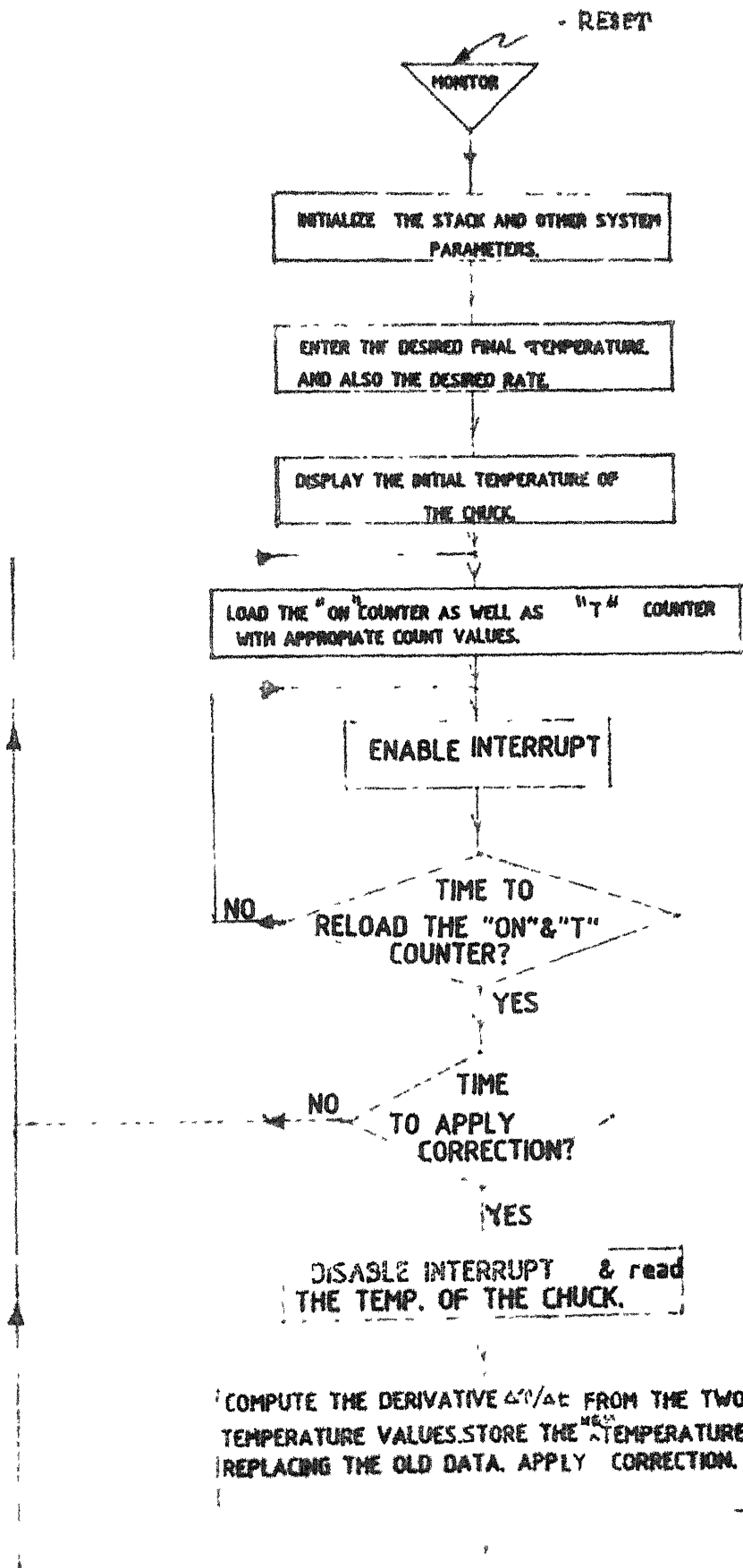
Refer to the flow charts in Figs. 3.6 and 3.7. The exact details of how the above 'algorithm' has been realized are given below.

(a) The programme, when executed, asks for entering the desired final temperature at which cross-over from ramp mode to constant temperature mode should take place. This is followed by another request to enter the desired ramp rate (between $20^{\circ}\text{C}/\text{min}$ and $90^{\circ}\text{C}/\text{min}$).

(b) Depending on the desired ramp rate, the 'ON' counter is loaded by some 'count' value equal to some integral number of a.c. cycles for which power should be applied to the load. Another counter known as 'T' counter also gets loaded by the total number of a.c. cycles chosen per group. The ratio of this 'ON' counter to 'T' counter is the duty cycle of power to be applied to the load. 'Duty Cycle' is varied by varying the count value loaded into the 'ON' counter.

(c) The interrupt system is enabled. As discussed earlier, the interrupts come after every 20 msec. i.e. time for one full a.c. cycle. The programme keeps waiting till the occurrence of interrupts.

(d) When interrupted, the programme jumps to Interrupt Service Subroutine and performs the following operations:



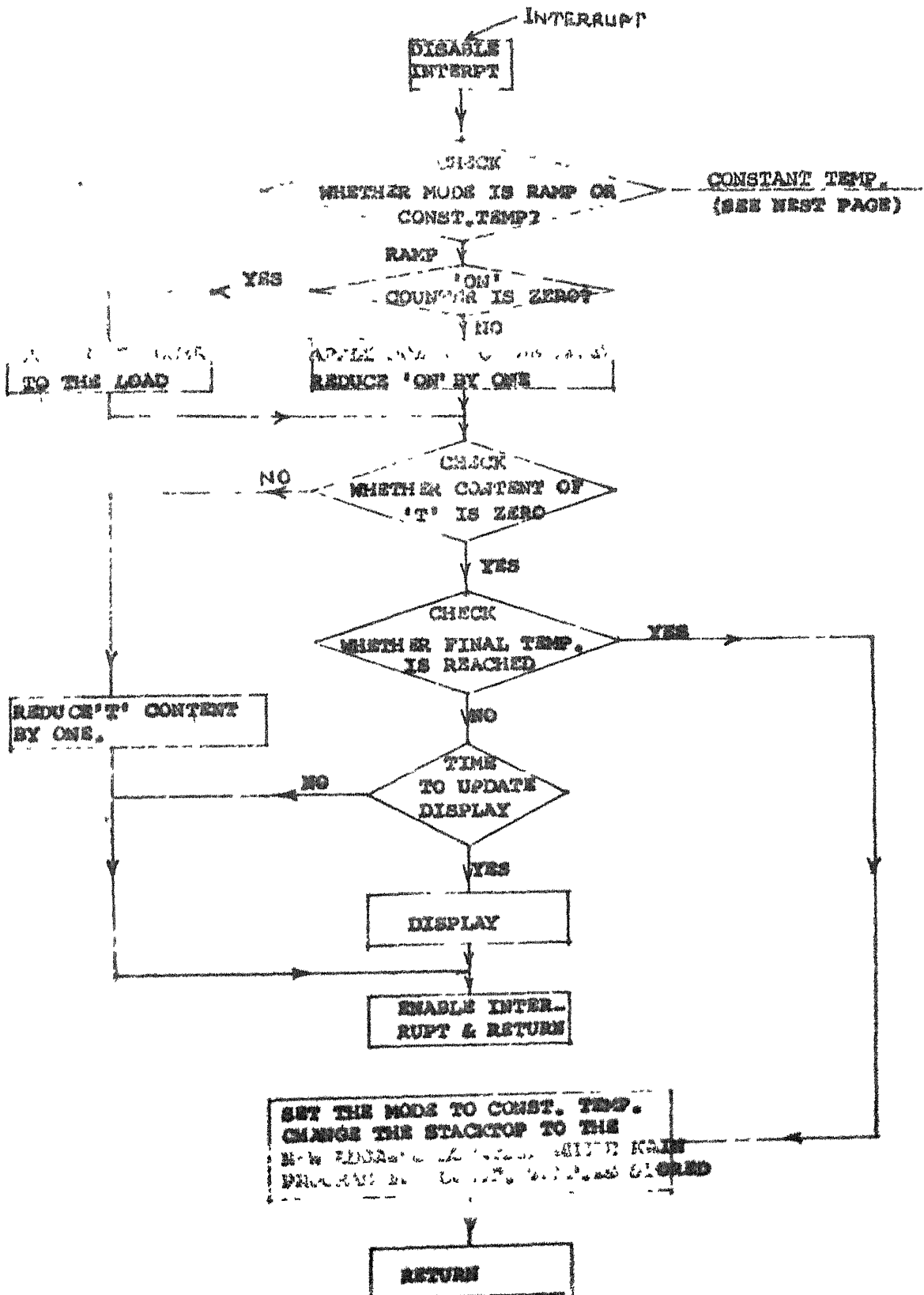


FIG. 3.7 IAS PROGRAMS FOR RAMP MODE

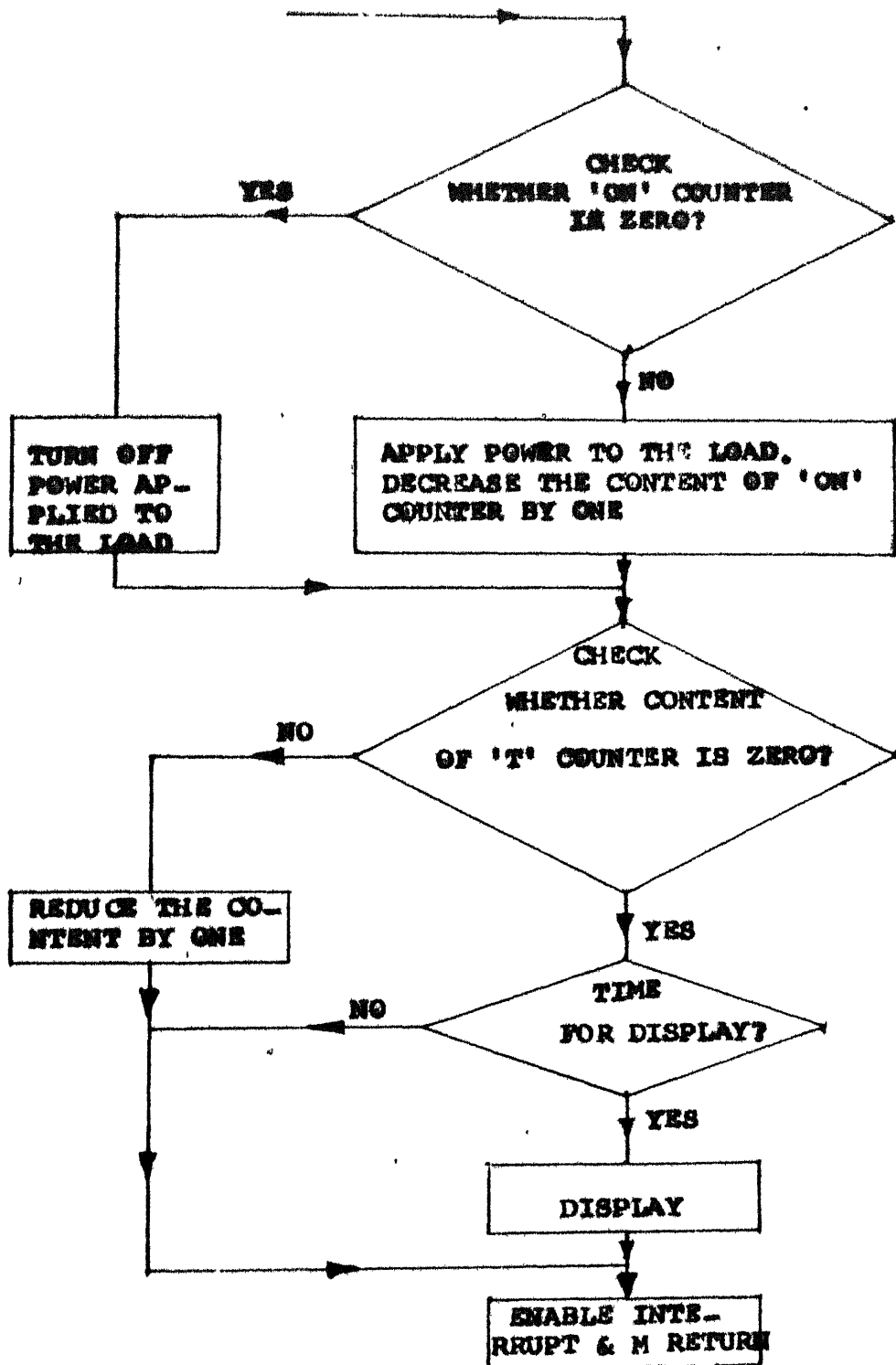


FIG. 3.7 (CONTINUED) ISS PROGRAMME FOR CONST. TEMP. MODE.

1. Checks first whether 'Mode' is 'ramp' or 'constant temperature'?

If 'mode' is found to be 'constant temperature', the programme branches off to some location within the ISS itself. This location contains programme written for 'constant temperature mode'.

If 'mode' is found to be 'ramp', it proceeds to follow the next instructions.

2. A check is made regarding the contents of the 'ON' counter. If content of 'ON' counter is non-zero, power needs to be applied to the load. This is done by sending a logic '1' to the I/O port pin A_0 of 8255P-2, which in turn controls the gate signal of the control thyristor Q_1 of the A.C. power controller (Fig. 3.2). In addition to the above task, content of 'ON' counter is decreased by one.

If content of 'ON' counter is found to be zero, power to the load needs to be switched off. This is done by sending a logic '0' to the I/O port pin A_0 .

3. Having checked the 'ON' counter, content of 'T' counter is also checked and decreased by one.

4. The temperature of the thermochuck is measured with the help of A/D converter and compared with the desired final temperature.

If the final temperature is reached, two jobs are done,

- a) 'Mode' is set to 'constant temperature Mode'
- b) The stacktop, which stored the main programme address before entering ISS, is changed to some new address location, where main programme for 'constant temperature mode' is written.

If final temperature is not reached, programme proceeds to the next instruction.

5. A check is made whether time to update display of chuck temperature is reached or not. If display time is 'up', a 'display routine' is called. If not, programme comes out of the ISS and goes back to the main programme again.

e) After ISS is served, the programme while waiting for the next interrupt to come, carries out a routine check, whether content of 'T' counter (which gets decreased by one, each time an interrupt occurs) is reduced to zero or not.

If yes, again one more check is made whether the time for applying 'correction' is reached or not?

If 'correction' time is yet to come, the programme goes back to step (b). The 'ON' counter and also the 'T' counter gets reloaded with the previous cycle values and the whole sequence repeats.

If 'correction' time is 'up', a 'correction routine' is called. The temperature of the chuck is recorded. From two temperature readings, (the last reading was taken during the last 'correction' interval), the derivative $\frac{\Delta T}{\Delta t}$ is calculated and compared with the desired $\frac{\Delta T}{\Delta t}$. Depending on the amount and direction of error, a correction is applied which results in either increase or decrease of count values in the 'ON' counter. With this new count value, the programme jumps back to step (b) and the entire sequence repeats.

(f) The main programme and also the ISS written for constant temperature mode is quite simple. The system can remain in the constant temperature mode for an infinite period of time, unless reset by pressing the 'reset' button of the keyboard.

3.3.2 Hyperbolic Mode:

The 'algorithm' used for generating hyperbolic heating rate schedule is merely an extension of the 'algorithm' used for generating ramp mode itself. The non-linear equation of

the form $\frac{1}{T} = \frac{1}{T_0} - at$, used for generating hyperbolic heating rates, can be approximated in a piecewise linear fashion. Differentiating the equation with respect to time we get,

$$\frac{dT}{dt} = aT^2 \quad (3.2)$$

i.e. the rate of rise of temperature at any instant is proportional to the square of ^{the} temperature at that instant. Therefore, by computing rates of rise at regular short intervals of time and by employing the 'algorithm' used for ramp mode of heating, one can easily and fairly accurately approximate a hyperbolic heating rate schedule.

Two problems become obvious.

- a) We already pointed out that, at very low ramp rates (less than 20°C/min), the heater's response is very poor, mainly because of losses. To start with, computed rates from eqn. (3.2) may become very small and heater's inability to respond faithfully at these rates will result in error.
- b) When the temperature is very high, computed rates also may become very high, even higher than the maximum rate (90°C/min) above which, the heater can not respond. This imposes another limitation.

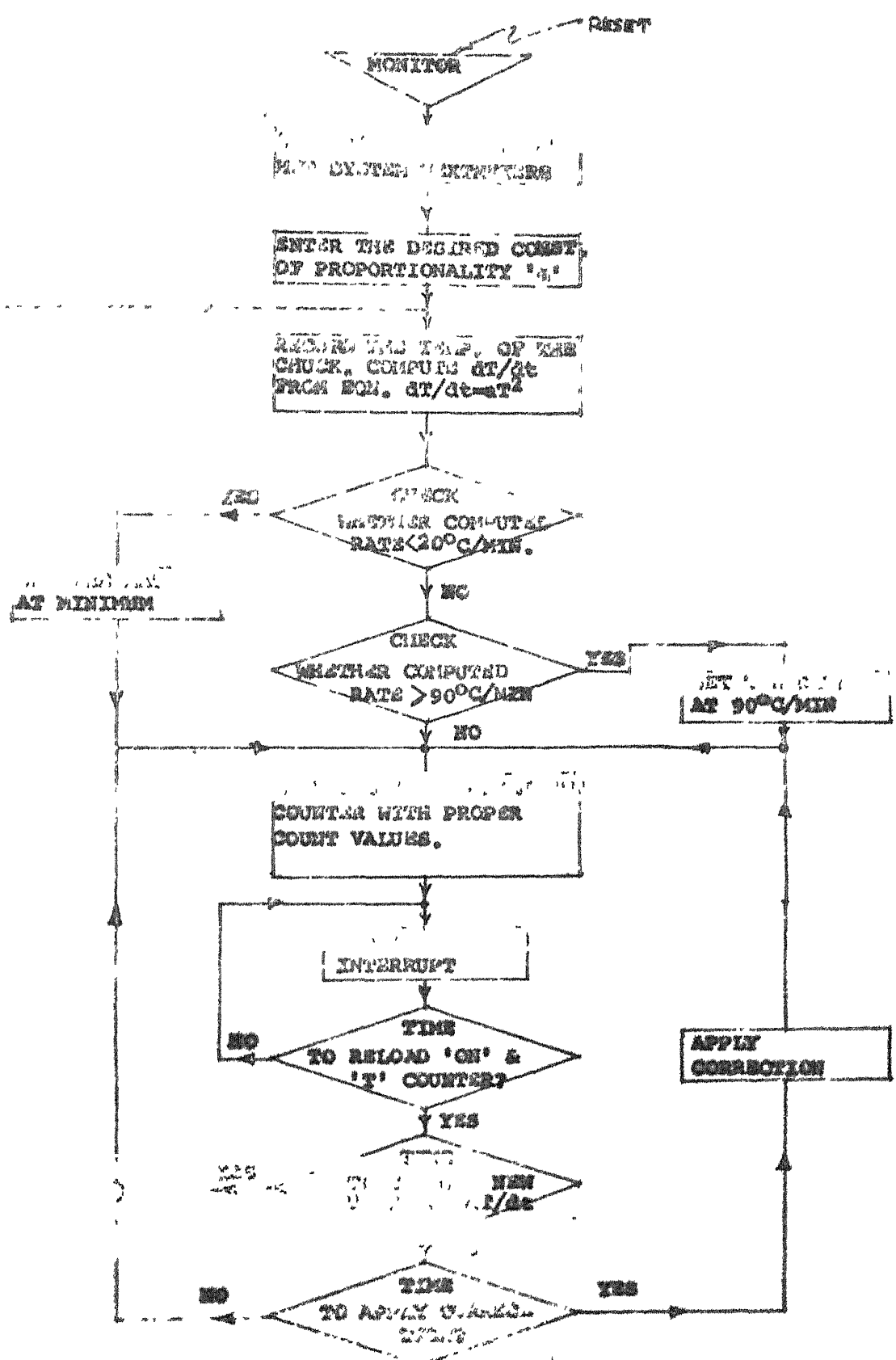


FIG. 3.6 MAIN PROGRAMME FOR HYPERBOLIC HEATING RATE

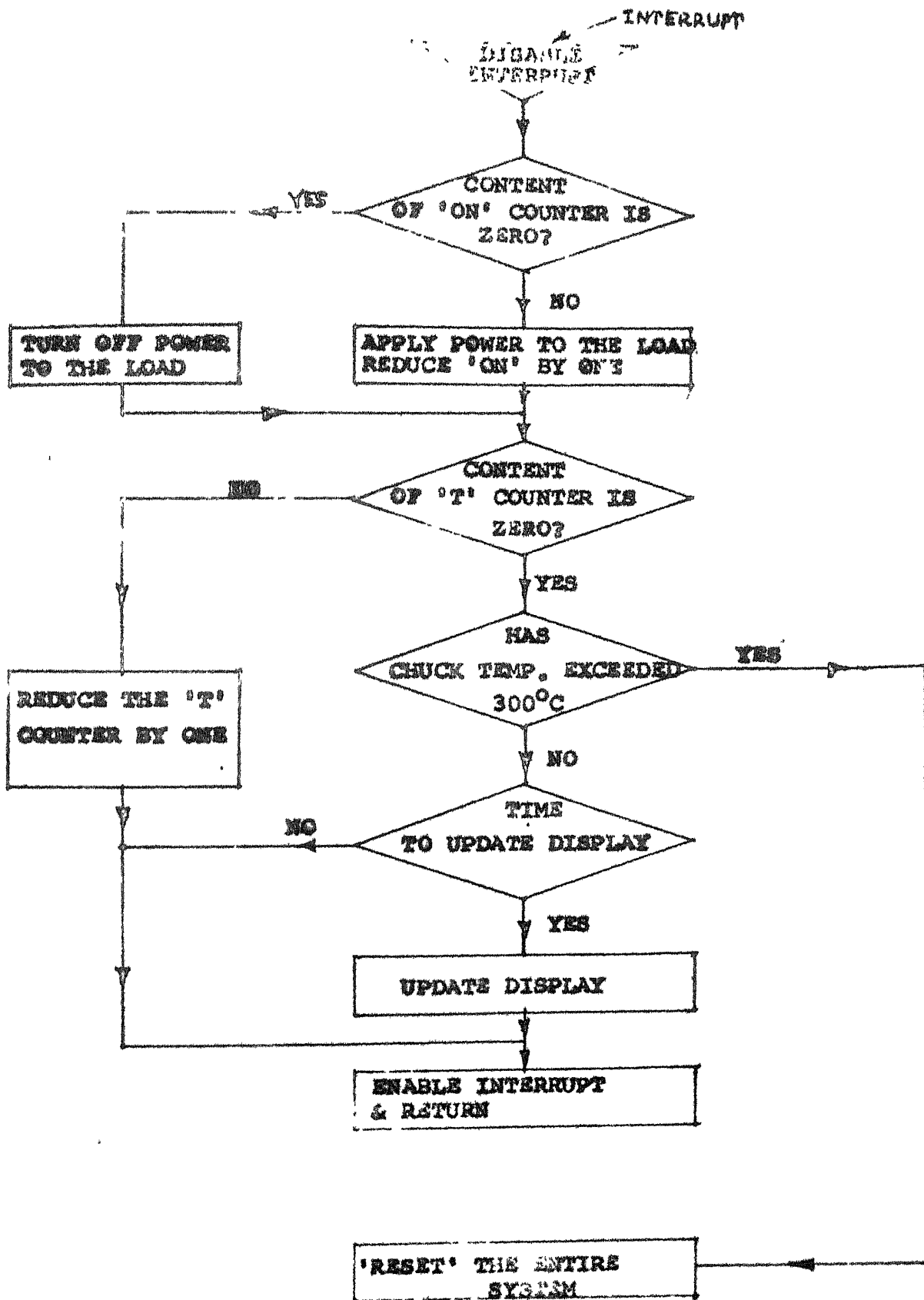


FIG. 3.9 ISS PROGRAMME FOR HYPERBOLIC HEATING RATE

Refer to the flow charts shown in Figs. 3.8 and 3.9. The details of the algorithms are given below:

1. When executed, the programme asks for entering the desired value of the constant of proportionality 'a'.
2. The chuck temperature is read and recorded. The derivative $\frac{dT}{dt}$ at that instant is computed from eqn. (3.2) with the desired 'a' value.

If this computed value becomes less than the minimum ramp rate $\frac{dT}{dt}$ till which the heater responds satisfactorily, a 'threshold' or minimum heating rate is ensured for the heater. If the computed value becomes more than the 'threshold' heating rate, the heater is heated up at that rate only. On the other hand, if computed rate becomes greater than $90^{\circ}\text{C}/\text{min}$, the heater is heated at $90^{\circ}\text{C}/\text{min}$ only.

3. Depending on the rate, the 'ON' counter is loaded by some count value equal to some integral number of a.c. cycles for which power should be applied to the load. Another counter known as 'T' counter also gets loaded by the total number of a.c. cycles chosen per group. The ratio of this 'ON' counter to 'T' counter is the duty cycle of power to be applied to the load. 'Duty Cycle' is varied by varying the count value loaded into the 'ON' counter.

4. The interrupts of the system are enabled. The system keeps waiting till the occurrence of the interrupts.

5. When interrupted, the system jumps to Interrupt Service Subroutine. It does the following functions there:

- a) Checks whether 'ON' counter content is zero or not? If non-zero, power is applied to the load and also 'ON' counter content is decreased by one. If zero, power to the load is switched off.
- b) Having checked the 'ON' counter, content of 'T' counter is also decreased by one.
- c) The temperature of the chuck is measured and is compared to the value of 300°C , the temperature beyond which the heater should not be operated. If the measured temperature is found to exceed 300°C , the system is switched off; otherwise proceeds to the next instruction.
- d) A check is made whether time to update display of chuck temperature is reached or not? If yes, 'display routine' is called to show the chuck temperature. If not, the programme comes out of the ISS and returns to the main programme.

6. After ISS is served, the programme while waiting for the next interrupt to come, carries out a check whether content of T counter, (which gets decreased by one, each time an interrupt occurs) is reduced to zero or not? If not, the system keeps waiting for the interrupt. If yes, again two checks are made:

- a) Whether time for computing new value of $\frac{dT}{dt}$ is reached or not? If yes, the system jumps back to step (2) and the entire sequence repeats. If no, proceeds to the next instruction.
- b) Whether time for 'correction' is reached or not? If not, reload the 'ON' counter and 'T' counter with the previous count values, and a new load cycle starts. If yes, 'correction' is applied and the 'ON' counter is loaded with the corrected count value. 'T' gets loaded with the usual old value. Now the entire sequence from step (4) repeats.

Chapter 5 gives an analysis of the results obtained by operating the temperature controller for generating both linear as well as hyperbolic profiles.

CHAPTER 4

EXPERIMENTAL DETERMINATION OF MOBILE ION CONTAMINATION IN MOS CAPACITORS

Even in the early days of MOS technology, it was universally experienced that mobile sodium ions in the oxide were responsible for the drift in device characteristics. Apart from the identification of most common sources of sodium, the importance of introducing 'monitoring' at various steps during fabrication of the devices, was felt. Sensitive electrical measurements as well as elaborate theoretical models (connecting the behaviour of the ions to the measurements) have been developed. The resulting knowledge has been used to minimize or eliminate sodium contamination during manufacture.

In this chapter, an experimental technique for determining the density of Mobile ion contamination in MOS capacitors has been described. The experiment has been carried out using commercial instruments like C-V plotter, Thermochuck, Temperature Controller (all made by Princeton Applied Research) and a X-Y recorder (made by Hewlett Packard).

4.1 EXPERIMENT:

The device chosen for carrying out the experiment is a MOS capacitor, having n-type silicon. Fig. 4.1 shows the structure of the device. Basically, it is a parallel plate capacitor, with one electrode a metallic plate, known as 'gate' and the other electrode, the silicon (n type), separated by a thin insulating layer of SiO_2 .

The method adopted for finding out sodium ions is the widely used C-V method, where a plot of high frequency (1 MHz) C-V curves of the MOS capacitor are taken after bias-temperature variations.

The sources of capacitance in MOS capacitor are well known [11]. As shown in Fig. 4.2, it comprises basically of a fixed insulating layer capacitance (C_i) in series with a variable capacitance of the semiconductor C_s . For an n-type silicon, as gate bias is swept from a positive value , through zero, to a negative value , the device passes through an 'accumulation' to 'depletion' to onset of a 'strong inversion'. The resulting differential capacitances associated with the device, have been shown in Fig. 4.3, as a function of gate bias voltage. The curve (a) is \int^{the} 'high-frequency C-V curve' of the device whereas curve (b) is the 'low-frequency' C-V curve.

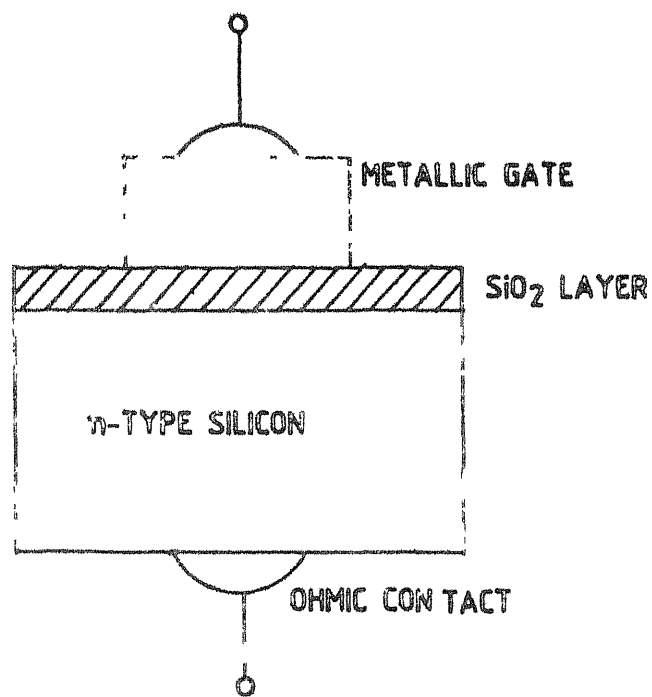


FIG.4.1 STRUCTURE OF a n-TYPE MOS CAPACITOR.

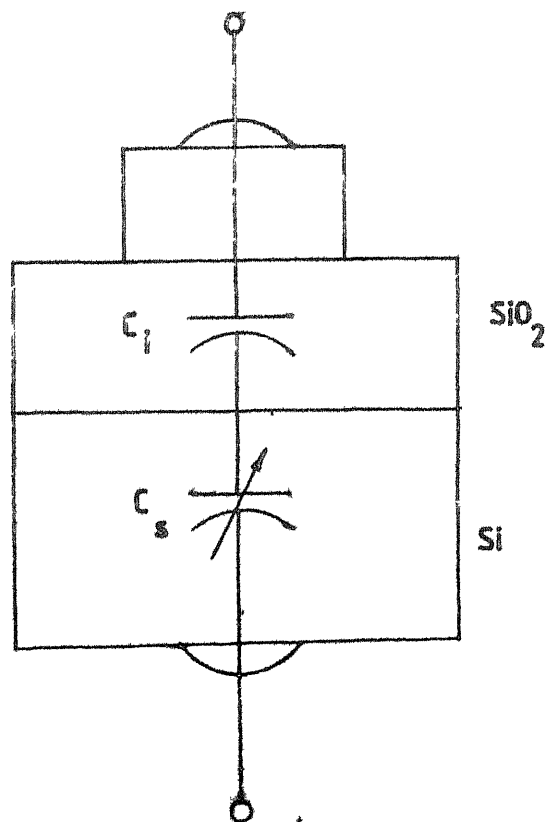


FIG.4.2 CAPACITANCES ASSOCIATED WITH n-TYPE MOS CAPACITOR.

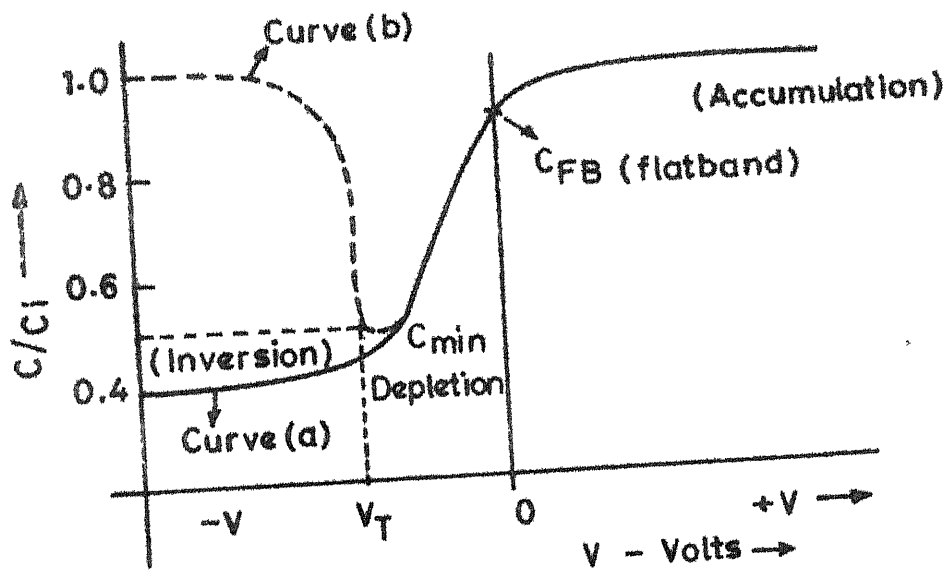


FIG.4.3 High Frequency as well as Low Frequency C-V curves of MOS Capacitors .

The experimental set-up for determining the density of mobile ion contamination has been shown in Fig. 4.4. The PAH (Princeton Applied Research) model -410 C-V plotter alongwith Thermochuck/Temperature controller and a micromanipulator probe station assembly, permitted a highly automated measurement.

The steps of the experiment were as follows:-

a) First, a high frequency C-V curve of the DUT was plotted on a graph paper (Fig. 4.5) by means of the X-Y plotter. 'Start' voltage of the programmable ramp generator of the 'C-V plotter' was front-panel adjusted to a value of 3.5 volt whereas 'Stop' voltage was kept at -5 volt. 'Ramp-Multiplier' and 'Ramp Rate' were kept at 10 and 50 mv/sec respectively.

b) The initial C-V plot being over, a positive bias stress of about 30v was applied to the device. The device was now heated up to a temperature of 190°C , with the bias stress applied throughout the temperature cycle. After the temperature reached the desired value of 190°C , the device was held up there for a period of about 5 mins., enough time to ensure that all of the sodium ions, drifted across the oxide layer.

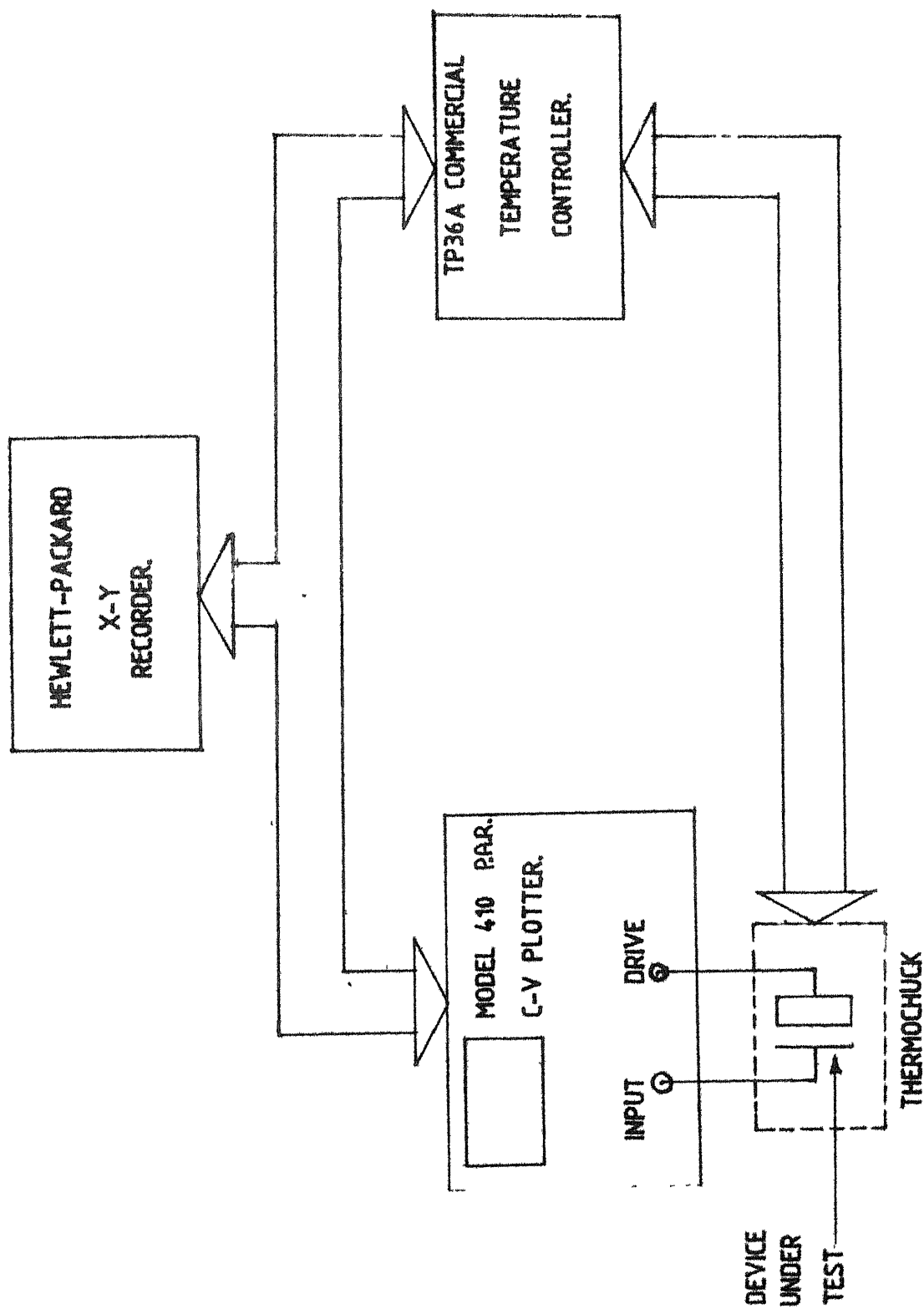


FIG. 4.4 EXPERIMENTAL SET-UP FOR DETERMINING THE DENSITY OF MOBILE IONS IN MOS CAPACITORS.

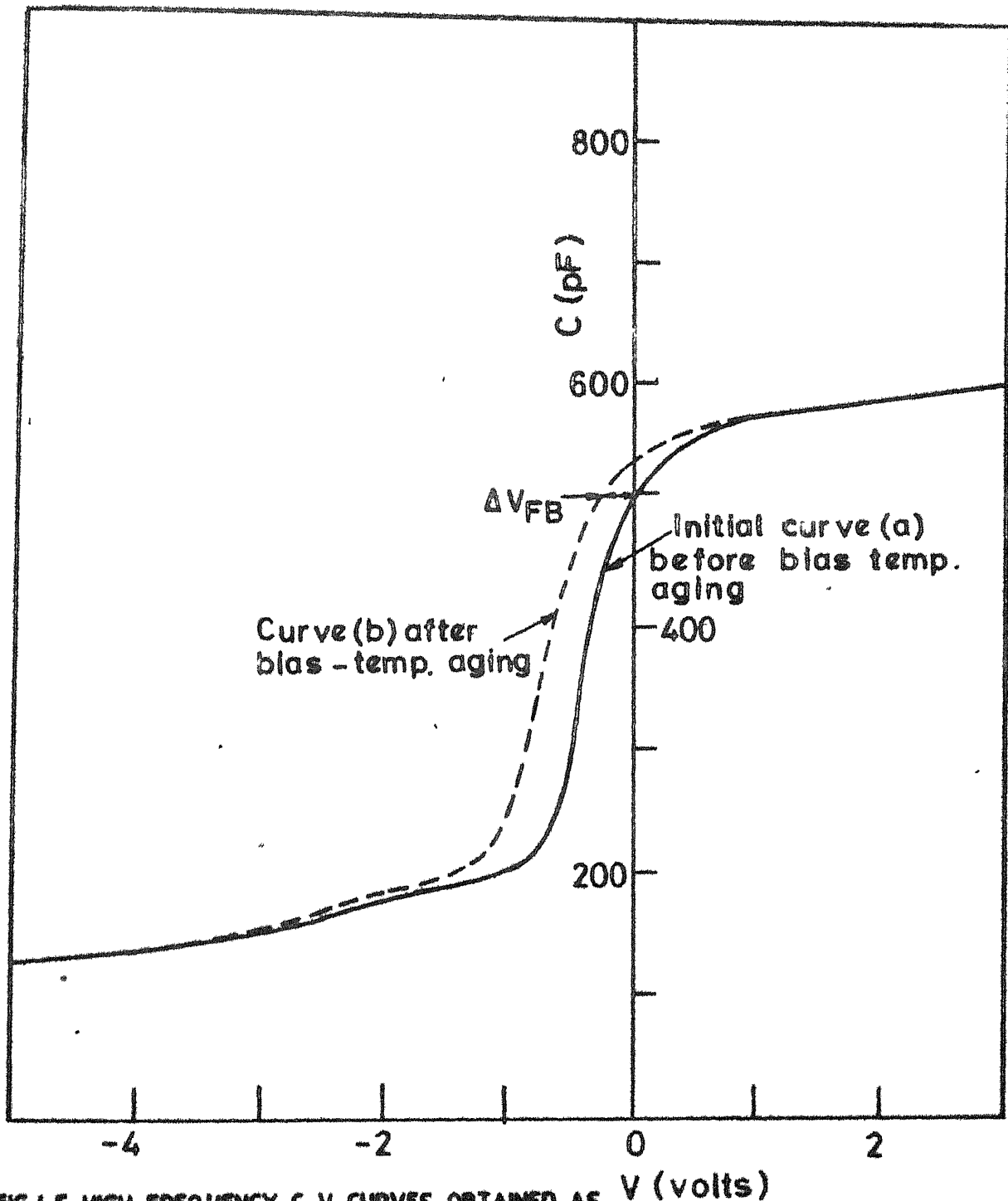


FIG.4.5 HIGH FREQUENCY C-V CURVES OBTAINED AS A RESULT OF BIAS-TEMPERATURE AGING.

c) After the given time period at elevated temperature and at high field, the device was cooled back to room temperature.

d) When it reached the room temperature another C-V plot of the MOS capacitor, was taken. The curve (b) in Fig. 4.5 is the second C-V curve obtained after bias/temp. aging of the device.

4.2 RESULTS AND DISCUSSION:

Fig. 4.5 clearly shows that the two high-frequency C-V curves are not identical. The second curve has actually shifted leftwards with respect to the first one. This voltage shift in C-V curve, known as 'flat-band shift' is a measure of the density of Mobile Ion contamination in MOS capacitors. The reason for this shift is the oxide charges, that exist in practical MOS devices. Before we digress into the discussion of reasons, the experimental results, that were obtained, are mentioned below.

at $V = 0$ the flatband capacitance was measured to be $= 510 \text{ pF}$.

The 'flatband voltage shift' ' ΔV_{FB} ' was measured to be $= 0.3 \text{ volt}$.

The density of Mobile Ions

$$= N_{ox} = \frac{\epsilon_0 K_{ox} \cdot \Delta V_{FB}}{q t_{ox}}$$

where N_{ox} = density of states, cm^{-2} , eV^{-1}

ϵ_0 = Permittivity of free space

$$= 8.854 \times 10^{-12} \text{ coulomb volt}^{-1} \text{ m}^{-1}$$

K_{ox} = Oxide dielectric constant (3.8 for SiO_2)

q = electric charge 1.6×10^{-19} coulomb

t_{ox} = Oxide thickness = 500 Å or $0.5 \times 10^{-7} \text{ m}$.

$$\text{or } N_{ox} = \frac{(8.854 \times 10^{-12})(3.8)(0.3)}{(1.6 \times 10^{-19})(0.5 \times 10^{-7})}$$

$$= 12.6 \times 10^{14} \text{ m}^{-2}$$

$$= 1.26 \times 10^{11} \text{ cm}^{-2}.$$

The ideal characteristics of MOS capacitors get affected by interface traps, oxide charges etc. that exist in practical MOS devices. The exact nature of Si-SiO₂ interface is not yet fully known. A picture of interface areas of MOS capacitor is shown in Fig. 4.6.

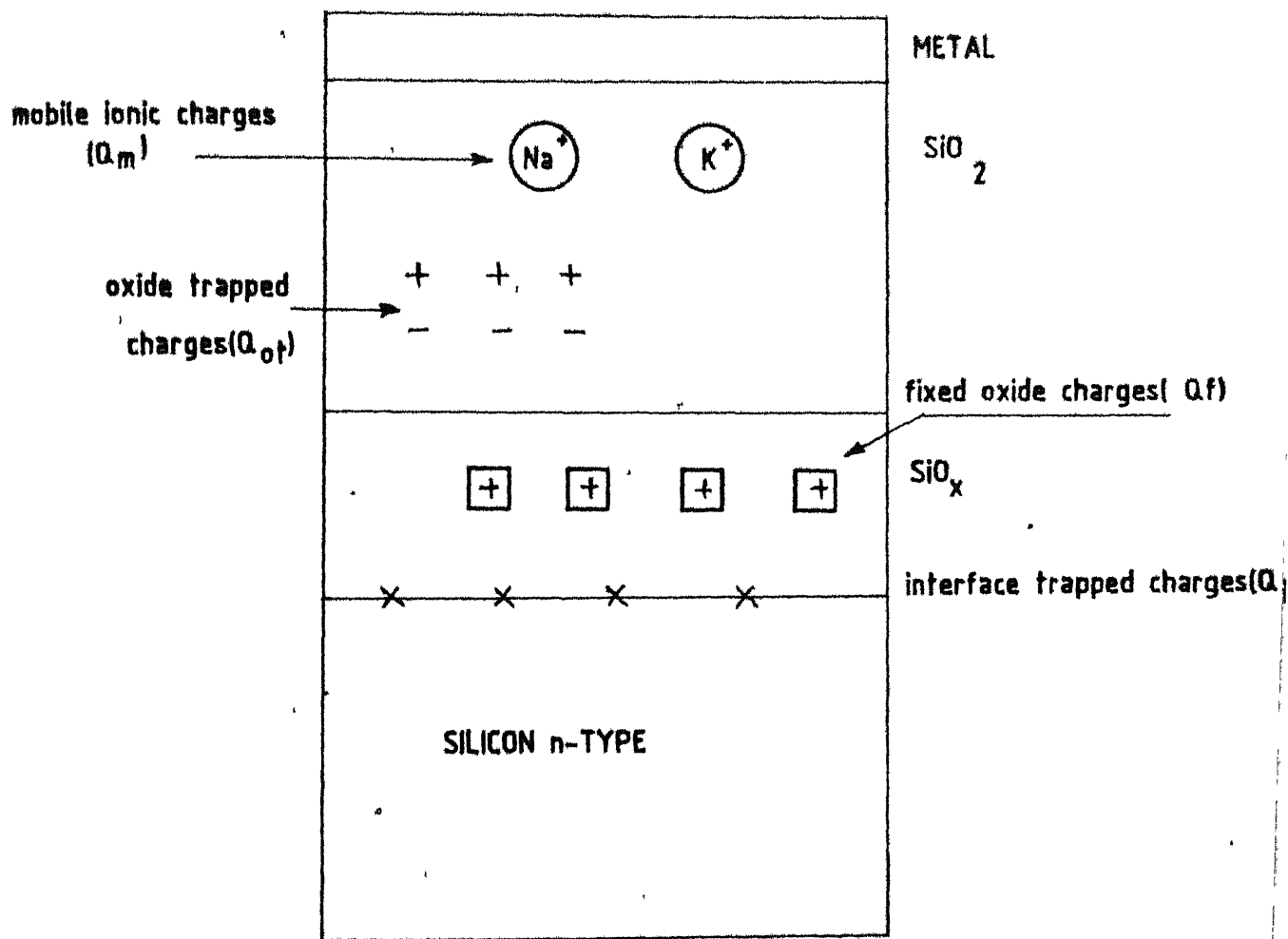


FIG.4.6 OXIDE CHARGES PRESENT IN PRACTICAL MOS CAPACITORS.

Two basic types of charges are found in SiO_2 layer.

- 1) Interface trap charges (Q_{it})
- and 2) Oxide charges (Q_o)

Oxide charges are further classified into three types.

- a) Oxide fixed charges (Q_f)
- b) Oxide trapped charges (Q_{ot})

and c) Mobile Ionic charges (Q_M), most commonly caused by the presence of ionized alkali metal atoms such as sodium, potassium etc. They are located either at Metal- SiO_2 or Si- SiO_2 interface, where it has drifted under an applied electric field.

A common manifestation of interface trap charges within a MOS-capacitor is the distorted or spread-out nature of the C-V characteristics. Experiments like bias/temperature aging can not be used to determine these charges [12]. There are other sophisticated methods, a detailed discussion can be obtained from reference [13].

The very fact that oxide fixed charges (Q_f) and oxide trapped charges (Q_{ot}) are immobile in nature and are independent of oxide thickness, semiconductor doping concentration and the semiconductor doping type (n or p), they cannot contribute to the shift in high frequency C-V curves as a result of bias/temperature aging. But, the

presence of these fixed charges results in a translation of the initial C-V curves towards negative biases, relative to the theoretical C-V curves [12].

Annealing in an inert atmosphere, is a standard procedure for minimizing the oxide fixed charges.

4.3 CONCLUSION:

The simple bias/temperature aging experiment for determining the density of Mobile Ion contaminations in MOS capacitors, does not depend on the nature of heating profiles, one follows, to heat up the device. We employed a commercial temperature controller to heat and cool the device. We could as well have used our microprocessor controlled temperature controller for the purpose; but the problem was that, our system did not have the facility to automatically initiate a cooling cycle.

87564

CHAPTER 5

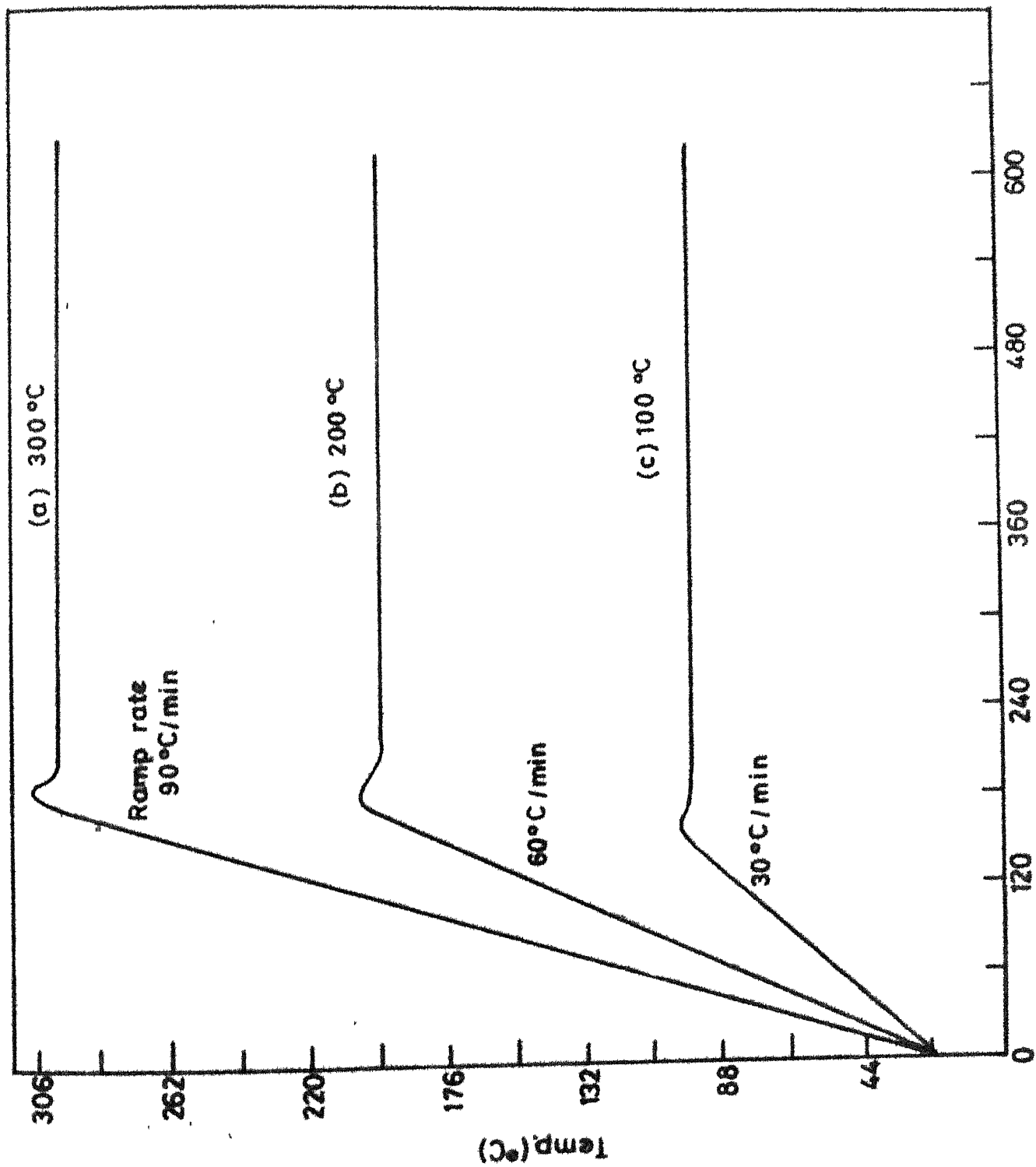
RESULTS AND DISCUSSION

A set of curves for both linear as well as hyperbolic heating rates (shown in Fig. 5.1 and Fig. 5.2) have been obtained, following the set of operating instructions mentioned in Appendix II. These curves show a plot of temperature (Y-axis) in $^{\circ}\text{C}$ vs. time (X-axis) in secs. They have been obtained with the help of a X-Y recorder, where Y inputs of the recorder have been fed with the amplified thermocouple output and X-inputs with the 'Ramp Output' of a programmable ramp generator.

In this chapter we will analyze the results obtained, the deviations from the expected values, the possible reasons for these discrepancies and lastly, the limitations of our system.

5.1 RAMP DATA:

Fig. 5.1 shows three curves [marked as (a), (b) and (c)] for three different ramp rates with three different final temperatures, at which cross-over from ramp mode to constant temperature mode has taken place. Curve (a) is for ramp rate of $90^{\circ}\text{C}/\text{min}$ with a switch over at 300°C . Curve (b), $60^{\circ}\text{C}/\text{min}$ with a switch over at 200°C and curve (c),



30°C/min with a switch over at 100°C. All the three curves originate from ambient temperature itself.

Apart from a T-t plot by means of X-Y recorder, a set of actual temperature data were taken for all the three curves. They were displayed by the seven segment display of the microprocessor kit at a regular interval of 10 secs. This display helped in tracking the performance of the system. As expected, there are discrepancies in the beginning before the 'correction routine' starts functioning and in the end, due to thermal inertia. These points are evident in the data for curve (a), shown in Table I. Table II and Table III show similar data for curves (b) and (c) respectively.

From the three tables and also from Fig. 5.1 it is evident that the results are in agreement with the desired rate of rise of temperature. The slight undulations seen in constant temperature mode are expected, because in constant temperature mode, the system employs normal 'Proportional Control' technique. The maximum temperature rate attainable was 90°C/min. The heater can not respond faster than this. The lower limit was found to be 20°C/min. This limit was dictated by the fact that at very low duty cycle of applied power the losses from the heater

Table I

Initial Temperature = 22°C Desired Ramp rate = $90^{\circ}\text{C}/\text{min}$.Desired Final Temperature = 300°C

Time interval of measurement = 10 sec.

Time in sec.	Actual Temp. in $^{\circ}\text{C}$	Increment ΔT in every 10 secs.	Remarks
0	22°C	-	Rate/min= 84°C Error = $-6^{\circ}\text{C}/\text{min}$
:	:	:	
:	:	:	
30 sec.	64°C		Rate/min = 92°C Error = $+2^{\circ}\text{C}/\text{min}$
40 sec.	78	14°C	
50 sec.	93	15°C	
60 sec.	109	16°C	
70 sec.	124	15°C	
80 sec.	140	16°C	
90 sec.	156	16°C	
:	:	:	Rate/min = 92°C Error = $+2^{\circ}\text{C}/\text{min}$
:	:	:	
120 sec.	202	:	
:	:	:	
180 sec.	294	.	

Table II

Initial Temperature = 24°C
 Desired rate = $60^{\circ}\text{C}/\text{min}$
 Desired Final Temperature = 200°C
 Time interval of measurement = 10 sec.

Time in sec.	Actual Temp. in $^{\circ}\text{C}$	Increment ΔT in every 10 secs.	Remarks
0	24°C	-	Rate/min. = 56°C Error = $-4^{\circ}\text{C}/\text{min}$.
:	:		
:	:		
60 sec.	80°C		Rate/min = 61°C Error = $+1^{\circ}\text{C}/\text{min}$
70 sec.	90°C	10°C	
80 sec.	100°C	10°C	
90 sec.	110°C	10°C	
100 sec.	120°C	10°C	
110 sec.	130°C	10°C	
120 sec.	141°C	11°C	Rate/min = 63°C Error = $+3^{\circ}\text{C}/\text{min}$
:	:	:	
:	:	:	
:	:	:	
180 sec.	204°C	.	

Table III

Initial Temperature = 23°C Desired Rate = $30^{\circ}\text{C}/\text{min}$ Desired Final Temperature = 100°C

Time in sec.	Actual Temp. in $^{\circ}\text{C}$	Increment ΔT in every 10 secs.	Remark
0	23°C	-	Rate/min = 26°C Error = $-4^{\circ}\text{C}/\text{min}$
:	:		
:	:		
30 sec.	36°C		Rate/min = 32°C Error = $+2^{\circ}\text{C}/\text{min}$
40 sec.	41°C	5°C	
50 sec.	46°C	5°C	
60 sec.	51°C	5°C	
70 sec.	57°C	6°C	
80 sec.	62°C	5°C	
90 sec.	68°C	6°C	Rate/min = 31°C Error = $+1^{\circ}\text{C}/\text{min}$
:	:		
:	:		
150 sec.	99°C		

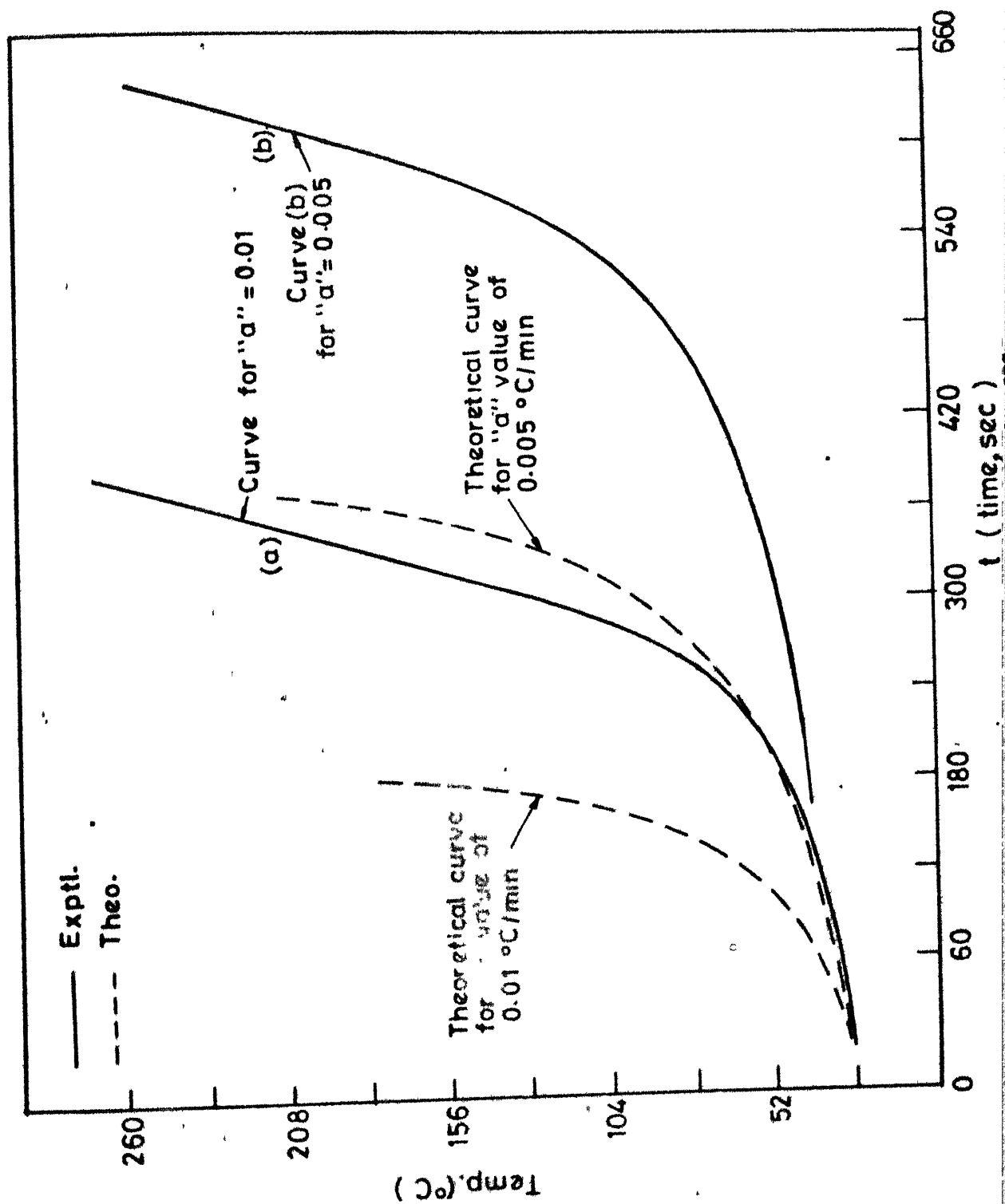
system become so predominant that the thermal response becomes highly non-linear.

5.2 HYPERBOLIC DATA:

A hyperbolic heating rate in accordance with the equation $\frac{1}{T} = \frac{1}{T_0} - at$, was generated by approximating the non-linear equation in a piecewise linear fashion. By differentiating the equation with respect to time, it can be shown that rate of rise of temperature at any instant is proportional to the square of the temperature at that instant (i.e. $\frac{dT}{dt} = aT^2$). Therefore, by computing rates of rise at regular, short intervals of time and by employing ramp mode of heating, one can easily and fairly accurately approximate a hyperbolic heating rate schedule.

Fig. 5.2 shows four curves. The two thick curves are the two actual hyperbolic curves generated for two different values of 'a'. Curve (a) is for 'a' value of 0.01 and curve (b) for 0.005. The other two dotted curves are the corresponding theoretical curves obtained by calculating the temperature values in accordance with the equation $\frac{1}{T} = \frac{1}{T_0} - at$.

It can be seen that, the theoretical and the practical curves are different. Though the curve shapes



are similar, the latter seems to have a horizontal shift across X-axis with respect to the former one. The reasons are:

1. Approximations that have crept in, in following piecewise linear technique.
2. As mentioned in case of Ramp Data, the thermochuck system shows a highly non-linear response at very low duty cycle mainly, because of losses. It takes a significant amount of time for the heater to change temperature even by 1°C . Therefore, we ensured a minimum heating rate for the system. If the computed rates become less than this minimum, the heater will be heated at the minimum rate only. This is an important reason of discrepancy between the theoretical and the actual curves. This also explains why the actual curves got shifted horizontally with respect to the theoretical ones.
3. When computed rates become higher than $90^{\circ}\text{C}/\text{min}$, the thermal system can not respond at those rates. This is another source of error. This explains why the two curves (a) and (b) with two different values of 'a', are parallel to each other at the upper ends.

5.3 LIMITATIONS:

The present temperature controller suffers from certain limitations. They are enumerated below:

1. The present controller does not have the facility to initiate a cooling cycle automatically. Right now we cool down the system manually by opening a stop-cock valve of the water supply duct connected to the thermochuck systems. The 'commercial temperature controller' used in bias/temperature aging experiments, does have a solenoid operated valve which is actuated automatically whenever a cooling cycle is required.

2. An important drawback in our A.C. power controller is that, under normal circumstances, when no power should be applied to load, the control thyristor (Fig. 3.2, Chapter 3) Q_1 needs to be conducting continuously. As discussed earlier, conduction of Q_1 shunts away the gate current of master thyristor Q_2 , thereby preventing a.c. power to be applied to load. This quiescent condition of Q_1 is not desirable in the sense that, if Q_1 fails to conduct due to any reason, the thermochuck will be heated up continuously and may ultimately get damaged if maximum temperature is exceeded.

3. The 'dwell-on' time at constant temperature mode (at the end of which cooling cycle should be initiated) can not be programmed in our temperature controller. The 'time' is now practically infinite. Whenever cooling of the system is desired, the system is reset first and then a stop-cock valve is opened manually to circulate cold water around the chuck.

4. 'Duty cycle modulation' technique for controlling load power in the A.C. power controller, introduces an important limitation; that is, coarseness or step size in controls. Change in the content of 'ON' counter, even by 1 count corresponds to a change of 2% in duty cycle. This again amounts to a change in rate of rise value by about $2.7^{\circ}\text{C}/\text{min}$. The resolution in duty cycle can be increased by increasing the number of a.c. cycles per group (i.e. the content of 'T' counter), but at the cost of sluggish thermal response.

5. Another limitation arises out of the various binary multiplication and division subroutines in our software. At present these routines can not take care of fractions etc.

6. The system needs to be calibrated, at least once, because of the presence of thermocouple and its associated cold-junction compensation etc. Once calibrated, it can be used for a long time.

CHAPTER 6

CONCLUSION

A simple and versatile microprocessor controlled temperature profile generator has been studied in this thesis. The controller has been designed to generate two types of temperature profiles

- a) ramp rate with a switch-over facility to 'constant temperature' mode,
- and b) Hyperbolic rate ($\frac{1}{T} \alpha t$)

The performance of the temperature controller is excellent in Type (a) heating. In case (b), even though the profiles generated are quite smooth and hyperbolic in nature, they are a bit inaccurate, owing to the thermal limitations of the heater system.

Compared to a 'Commercial Temperature Controller', our system has several advantages:

1. Capability of generating programmed heating profiles, particularly non-linear heating profiles.
2. Setting of the 'Final Temperature' at which cross-over from 'ramp' mode to 'constant temperature' mode takes place. One does not have to continuously adjust the setting of 'HIGH TEMP' potentiometer during the heating cycle, as in case of a 'commercial controller'.

3. In our controller, practically, there is no time limit to the 'dwell-on' time in 'constant temperature mode'. No precision mechanical timer etc. is required as in case of commercial ones. A simple manipulation of software can give any amount of 'dwell-on' time, one desires. (Our present system, right now, does not have the facility to programme 'dwell-on' time).

4. In constant temperature mode, the temperature of the system can be maintained within a very tight tolerance, ($\pm 1^{\circ}\text{C}$) which the commercial controllers are not capable of.

5. The heating of the system, is as desired, transient, and L.A.I. free. Two rugged and reliable thyristors supply a duty cycle modulated a.c. heating power to the chuck. Use of thyristors practically does not put any limitation to the power handling capability of the system. 'Commercial controllers' employ relays etc. for switching power to the load.

The advantages of our controller outweigh the few limitations, it suffers. And some of these limitations can be easily removed. However, the tremendous amount of flexibility and versatility that a microprocessor system provides, has not been fully exploited in the present work. All the drawbacks and limitations mentioned in the last

chapter can be easily removed at the cost of additional software and hardware complexity. For example, automatic initiation of cooling cycle can be easily provided by means of a solenoid operated valve acuated through one of the I/O port pins of ^{the} microprocessor kit. The user can be warned of the failure of control thyristor Q_1 in A.C. power controller by means of a simple alarm system. Software can be slightly modified to provide programmed 'dwell-on' time. Multiplication and Division routines can be written in a more elaborate way so that they can tackle fractions etc.

One can make an excellent T-t controller, by incorporating a few more non-linear profiles at the expense of little more software. The very fact that, we have an excellent ramp controller and any non-linear function can be approximated in a piecewise linear fashion, opens up the possibility of introducing some more non-linear heating profiles.

The thermal response of the chuck system can be bettered by enclosing it in a vacuum enclosure. This will reduce the convection losses etc. to a great extent. At present the chuck operates between ambient and 300°C , which can be further extended to a lower temperature limit of liquid nitrogen.

Apart from the control functions performed by the microprocessor, it can be pretty well extended to provide automated measurement capability. A variety of data can be read in by the microprocessor and can be used for further computation, for extracting various useful parameters required to characterize the semiconductor devices.

APPENDIX I

CALIBRATION PROCEDURE OF THE THERMOCOUPLE AMPLIFIER CIRCUIT FOR COLD-JUNCTION COMPENSATION

It was pointed out in Chapter 3 in connection with a discussion about amplifier circuitry (shown in Fig. 3.4) that, the amplifier needs to be calibrated, at least once, before the temperature controller is put into commission. Once calibrated, it need not be touched for a long period of time. This calibration is necessary, because the amplifier provides a kind of cold junction compensation for the thermocouple.

The simple calibration procedure is given below:

- a) Switch on the power supplies (i.e. +15v, -15v etc.
- b) Connect the Digital Multimeter (Keithley) at the output of LM308. Two lead-outs have been provided with the PCB for this ^{purpose.} \angle Display the voltage in 20v scale, D.C.V. The displayed reading when multiplied by 100 gives a straight measure of the temperature in $^{\circ}\text{C}$.

- c) Open the stop-cock of the water supply duct connected to the thermochuck and allow cold water to flow around the chuck. Allow this water circulation for some time. Note the temperature of the circulating water with the help of a thermometer.

d) Stop the water supply. Replace the thermocouple by a short of copper wire. Short the zener (shown in Fig. 3.4) to ground. Adjust the offset with the help of A3, 10K pot, till the LM308 output reads temperature of the circulating water at $10 \text{ mV}/^{\circ}\text{K}$. For example, if water temperature is found to be 25°C , output should read $(25 \pm 273) \times 10 \text{ mV}$, or 2.98 volts.

e) Remove the short across the zener but not across the thermocouple. Adjust the 5 K ohm potentiometer R9, to obtain output at $10 \text{ mV}/^{\circ}\text{C}$, i.e. for 25°C , output should read 0.25 volt.

f) Remove all the shorts, connect the thermocouple back. The circuit is ready for use.

APPENDIX II

OPERATING INSTRUCTIONS FOR THE TEMPERATURE CONTROLLER

For generating temperature profiles with the help of our temperature controller, the set of instructions that should be followed are:

1. Connect the two edge connectors properly to the PCB. The right hand side edge connector gets connected with the microprocessor kit, whereas the left hand side connector connects various power supplies (+5v, +15v, -15v etc.), thermocouple output, control lines of A.C. power controller etc. to the PCB.

2. Connect a digital multimeter (Keithley) at the output of LM 308 chip in order to monitor the chuck temperature. Two lead-outs have been provided at the top edge of PCB, to facilitate this connection. The multimeter should be set at 20V, DCV. The displayed voltage when multiplied by 100 gives a reading of temperature of the chuck in °C.

3. For getting a hard copy of the variation of temperature with time, a Hewlett-packard X-Y recorder is also connected to the system. The Y-inputs of the recorder are connected to the output of 741 op-amp, through another pair of separate lead-outs provided at the top edge of the PCB. The X-inputs

temperature of the cold water. Close the stop-cock and stop circulating water around the chuck. The system is now ready for the operation.

5. Switch on the 115v A.C. power supply. Under normal condition, the heater should not get power. The D.M.M., won't show any change in reading. The oscilloscope used to monitor the supply waveform^{and also the waveform} across the master thyristor Q_2 will show steady 50 Hz sine waves. When heater gets power continuously, the waveform across the thyristor Q_2 becomes a straight line.

6. Select the type of heating profile to be generated. If it is 'RAMP', store an instruction 'JMP 1A80' from RAM location FF~~7~~ of the microprocessor kit. If it is 'Hyperbolic' store 'JMP 1D20' from the memory location or 'FF~~7~~7'.

7. For RAMP mode, execute the programme from 1880H onwards. The steps are

- a) Press the button 'GO'. An arbitrary display 007D 3E will appear.
- b) Enter the address 1880 from the keyboard and then press execute button '.' of the kit.

- c) Seven-segment display will go blank. Enter the desired final temperature in three digits decimal form, i.e. if the desired temperature is ^{of} two digits, (XX) enter it as OXX. Please note that the maximum temperature is 300°C .
- d) The final temperature will be displayed twelve times followed by the display of a message 'PAE' again for twelve times. Enter now the desired rate in two digits decimal form. The maximum rate is $90^{\circ}\text{C}/\text{min}$. and ^{the} minimum is $20^{\circ}\text{C}/\text{min}$. Immediately after entering the desired rate, press the 'PLOT' button of C-V plotter to get a hard copy of T-t variation.

The thermochuck will be heated up in a linear fashion. The temperature of the chuck in $^{\circ}\text{C}$ will be displayed regularly at an interval of 10 sec. by the seven-segment display. The D.M.M. connected, will give a continuous reading of temperature

8. For 'Hyperbolic' mode, execute the programme from 1BBO II onwards. The steps are

(a) and (b) same as in (7).

c) A message 'PARA bL' will be displayed twelve times by the seven-segment display, after which the display will go blank. Enter now the value of the constant

of proportionality 'a' in two digits decimal form. Maximum value of 'a' to be entered is 10 (i.e. $0.01^{\circ}\text{C}/\text{min}$) and minimum value is 01 (i.e. $0.001^{\circ}\text{C}/\text{min}$). When the value of 'a' is entered, it will be displayed twelve times at the end of which press the 'PLOT' button. The hyperbolic heating rate will start. As in (7), the temperature of the chuck will be displayed regularly at an interval of 10 secs.

9. The programme be it 'RAMP' or 'Hyperbolic' can be stopped at any stage by pressing the 'RESET' button of the kit. For hyperbolic rate, if the temperature of the chuck exceeds 300°C , the system will be automatically 'reset'. For ramp rate, unless RESET button is pressed, the heater will remain at 'final temperature' indefinitely.

10. For cooling down the system, 'RESET' the system. Open the stop-cock valve and allow cold water to circulate. The temperature will start falling quickly. Keep an eye on the D.M.M. When chuck temperature reaches the ambient, close the valve.

The system is now ready for the next heating cycle. Repeat steps from (6).

Note that, one does not have to enter 'JMP ISS' instruction every time, unless one wants to change the mode of heating.

REFERENCES

1. R.Y. Koyama and M.G. Buehler, Rev. Sci. Instruments, Aug. 1979, p. 985.
2. G.A. Dussel and R.H. Bube, Physics Rev. 155, 764 (1967); R. Chen, J. Appl. Physics 40 (570), 1969.
3. P. Kelley and R. Braunlich - Phy. Rev. B1, 1587 (1970); P. Braunlich and P. Kelley, Phy. Rev. B1, 1596 (1970).
4. E.J. Schrenett; Journal of Scientific Instruments, 1242, 1968.
5. D. Mesweeney and P.W. Levy, Rev. Sci. Instruments, 36, 1324 (1965); Robert A. Wolf and Merle L. Bowser, Rev. Sci. Instrn, 38, 1806 (1967).
6. D.J. Buckley and G.E. Timbers, Rev. Sci. Instrm, 1972, July, 1018.
7. William L. Peterson, Rev. Sci. Instrm, vol. 46, No. 2, p. 196, Feb. 1975.
8. R.Y. Koyama and M.G. Buehler; Rev. Sci. Instruments, 50(8), Aug. 1979, p. 983.
9. SCR Manual, General Electric; SCR Manual Motorola Semiconductors.
10. National Semiconductor Handbook - Linear ICs
11. S.M. SZE, Physics of Semiconductor Devices.
12. Modular Series on Solid State Devices; Field Effect Devices - by Robert F. Pierret, p. 69.
13. J. Nicollian, MOS Devices, Physics and Experiments.

DATE SLIP

THIS book is to be returned on
the date last stamped.

[illegible]

EE-1985-M-MUK-MIG